U.S.G.S.

Reports open file Series.

accompanying (200)
R290
no 449

Weld - Int. 2548

UNITED STATES
DEPARTMENT OF THE INTERIOR
Geological Survey
Washington, D. C.

For Release JUNE 30, 1958

The Geological Survey is releasing in open files the following reports. Copies are available for consultation in the Geological Survey Library, 1033 General Services Bldg., Washington, D. C., and at other places as listed:

1. Geology of the Little Commonwealth area, Florence County, Wisconsin, by R. W. Johnson, Jr. 98 p., 20 figs., 2 tables.

   On file in Geological Survey offices, Room 213, Science Hall, Univ. of Wisconsin, Madison, Wis., and in Iron Mountain, Mich.

2. Pegmatite geology of the Shelby district, North Carolina, by W. R. Griffitts. 123 p., 31 figs., 4 tables.

449 3. The crystal structure of inyoite, by Joan R. Clark. 64 p., 19 figs., 14 tables.

x x x

THE CRYSTAL STRUCTURE OF INYOITE

Joan Robinson Clark

UNITED STATES GEOLOGICAL SURVEY

OPEN-FILE RELEASE

58-25

Open file reports

This report is preliminary and has not been edited or reviewed for conformity with Geological Survey standards and nomenclature.

Abstract

Inyoite, $CaB_3O_3(OH)_5.4H_2O$, is monoclinic, $\underline{P2_1/a}$, $\underline{a}$ = 10.63, b = 12.06, c = 8.405 Å (all ±0.020 Å), β = 114°02' ±5', Z = 4. The calcium location was obtained from identification of Ca-Ca vector peaks on the sharpened Harker section ($v = \frac{1}{2}$) and on the three sharpened Patterson projections. Positions for the remaining 15 atoms of the asymmetric unit were found by application of various "heavy-atom" techniques combined with known chemical and spatial requirements. Refinement was carried out from electron-density projections and difference syntheses. A 0.15 residual was obtained for each of the three principal zones. Inyoite contains the same isolated $[B_3O_3(OH)_5]^{-2}$ polyions that were found in meyerhofferite, $CaB_3O_3(OH)_5.H_2O$, and in the synthetic, $CaB_3O_3(OH)_5.2H_2O$. Such a polyion is formed by two BO_4 tetrahedra sharing a corner and one BO_3 triangle linking the two tetrahedra. Polyions of inyoite are connected to one another and to neighboring water molecules by bonding through calcium ions and by hydrogen bonds. Continuous polyion-calcium-water columns, oriented along lines parallel to [100], are thus formed. Adjacent columns are cross-linked chiefly by hydrogen bonding through water molecules. The observed cleavages, parallel to (001) and (010), break bonds only between columns.

Acknowledgments

It is a pleasure to acknowledge my indebtedness to all those who have assisted me in the course of this study. Special thanks are due to Dr. C. L. Christ, U. S. Geological Survey, for suggesting the problem and providing critical guidance, to Prof. J. D. H. Donnay, The Johns Hopkins University, for his continuing interest and counsel, to Dr. H. T. Evans, Jr., U. S. Geological Survey, who made the final drawing for Fig. 5 and gave valuable advice and encouragement, and to Dr. D. E. Appleman, U. S. Geological Survey, for helpful discussion. Calculations were processed by Mr. Vincent Latorre, Dr. D. E. Appleman and Dr. H. T. Evans, Jr., all of the U. S. Geological Survey. Inyoite crystals were kindly supplied by Dr. W. T. Schaller, U. S. Geological Survey.

Table of Contents

List of Tables

List of Figures

(Continued on next page)

List of Figures (Continued)

Introduction

Study of the crystal structure of inyoite was undertaken as part of an investigation of the calcium borate series, $2CaO.3B_2O_3.xH_2O$. This series includes the minerals colemanite, meyerhofferite, and inyoite, with x equal respectively to 5, 7 and 13; for x = 9 a synthetic compound is obtained which has not yet been found in nature. There are no other known members of the series. The crystal structure of colemanite has been described in detail (Christ, Clark and Evans, 1958) and preliminary accounts have been given for the crystal structures of meyerhofferite (Christ and Clark, 1956) and of the synthetic compound (Clark and Christ, 1957).

Inyoite was first described by Schaller (1916) from an occurrence in Inyo County, California, where it was found in close association with meyerhofferite and colemanite. It was noted then that meyerhofferite appeared as a pseudomorph of inyoite. Description of excellent crystals found in New Brunswick, Canada, was given by Poitevin and Ellsworth (1921). These authors confirmed and added to the data on crystallography, optics and chemistry previously given by Schaller. Other reported occurrences of inyoite and a summary of physical and chemical data are given in Palache, Berman and Frondel (1951).

Experimental Work

Crystal description, space group and cell dimensions

Crystals of artificial inyoite used for the structure study were prepared by W. T. Schaller by mixing 4ℓ of a saturated solution of gypsum, $Ca_2SO_4.2H_2O$, with 0.25ℓ of a saturated solution of borax, $Na_2B_4O_7.10H_2O$, and allowing the mixture to stand about nine months at room temperature. The space group, cell dimensions and x-ray powder data for inyoite were reported by Christ (1953); the space group and cell dimensions are repeated here.

Monoclinic; space group $\underline{P2_1/a}$ - $C_{\underline{2h}}^{\underline{5}}$ (No. 14)

$\underline{a}$ = 10.63, $\underline{b}$ = 12.06, $\underline{c}$ = 8.405 (all ±0.020 Å)

β = 114°02' ±5' (Moλ: $\underline{K\alpha}$ = 0.7107 Å; $\underline{K\alpha_1}$ = 0.70926 Å)

Cell contents: $4[CaB_3O_3(OH)_5.4H_2O]$

Density ($g.cm.^{-3}$): calc. = 1.873, obs. (Schaller, 1916) = 1.875.

The crystals are colorless, transparent, and of the general habit illustrated in Fig. 2 of Poitevin and Ellsworth (1921), i.e. tabular on {001}. While numerous forms have been observed on natural crystals, the synthetic crystals, measuring a few tenths millimeter per edge, exhibit only the following forms: dominant {001} and {110}, small {010}, occasional {111}.

Intensity measurements

X-ray equi-inclination Weissenberg patterns were taken with zirconium-filtered Mo radiation for seventeen layers about

[010] and for seven layers about [100]. For each exposure three films were interleaved with Ni foil 0.0005 in. thick in order to cut down the intensity from film to film. Exposures of about 72 hours at 50 kV and 20 mA were taken for each level; short exposures of about 2 hours each were also taken, when needed, to reduce the intensity of strong reflections to optimum reading range. Cu$\underline{K}\alpha$ radiation was used for recording low-angle reflections. All intensities were estimated visually by comparison with a standard spot strip. The n spots for the reference intensities on the standard strip were made from a given reflection of the inyoite crystal following the relation, $I_n = I_o(2)^{n/2}$, where I_o corresponded to a very faint blackening of the film. Excluding the space group absences, there are 5937 reflections contained in the sphere of radius $s = (\sin\theta)/\lambda = 0.9$ Å^{-1}. Of these, 3632 had $I > 0$, 2195 had I below the threshold of observation, and no observation was made for 110. Estimated intensities were converted to $F^2_{hk\ell}$ values by correcting for Lorentz and polarization factors, which were determined for each reciprocal lattice point as a function of cylindrical coordinates. Both IBM methods and the chart of Cochran (1948) were used to obtain the 1/Lp. No attempt was made to correct for variations in intensity readings due to shape effects on reflections occurring in upper-level Weissenberg films. Because the crystals were small no correction was made for absorption effects which were assumed negligible.

The intensities of the various levels were brought to the same relative scale by the use of appropriate film factors, based on comparison of intensity readings from different films for equivalent reflections. A range in scaled $F^2_{hk\ell}$ of one to 3000 was obtained. In order to arrive at a preliminary estimate of the temperature factor and of the factor required to convert the relative $F^2_{hk\ell}$ to an absolute scale, the K(s) curve described by Karle and Hauptman (1953) was constructed for inyoite (Appendix I). A set of absolute $F^2_{hk\ell}$ was obtained by multiplying the factor, K(0), into the relative $F^2_{hk\ell}$ values.

Other considerations

Throughout the analysis the observed and calculated structure factors were compared by using a scaling constant k, where $k\Sigma|F_o| = \Sigma|F_c|e^{-Bs^2}$. The method of Wilson (1942) was applied to determine the values of the average isotropic temperature factor, B. In the early stages of the calculations, atomic scattering curves for the neutral atoms, Ca and O, were taken from Viervoll and Ögrim (1949); for the final calculations, the values given by Berghuis et al (1955) were used. The atomic scattering factors taken for boron were those of Ibers (1957). At the present stage of refinement ionization states have not been taken into account. Maxima on the electron-density projections were calculated by the method of Booth (1948) for all resolved atoms.

Derivation and Refinement of Structure

The structural problem was to determine the coordinates for one calcium, twelve oxygen and three boron atoms, all in positions 4(e) of space group $\underline{P2_1/a}$ (International Tables, 1952). Although preliminary processing of three-dimensional data had been handled by IBM methods, machine facilities were not available either for three-dimensional series calculations or for Hauptman-Karle sign determination procedures. Therefore the structure derivation was begun by study of a Harker section, taken at $v = \frac{1}{2}$, and of three Patterson projections, each taken on a plane normal to a crystallographic axis (Appendix II). Each Fourier series was sharpened by taking coefficients, $p_{hk\ell}$, formed from the observed relative $F^2_{hk\ell}$ by correcting for both atomic form factor and thermal motion, as follows: $p_{hk\ell} = [K(s)\ F^2_{hk\ell}] \Big/ \hat{f}^2$, where $\hat{f} = \sum_{j=1}^{N} f_j \Big/ \sum_{j=1}^{N} Z_j$.

The sharpened Harker section for inyoite is shown in Fig. 1. Each of the sixteen atoms in the asymmetric unit is expected to give rise to two Harker peaks on this section, one at $u = \frac{1}{2}-2x$, $w = -2z$, and the other at $u = \frac{1}{2}+2x$, $w = 2z$. Each Ca-Ca Harker peak is expected to be about six times as large as an O-O Harker peak and about 2.5 times as large as any "non-Harker" Ca-O peak. Fig. 1 shows that the two largest peaks, labeled A and B respectively, actually have a ratio of about 2:1. By comparing each of these peaks, with respect to

both location and size, to peaks occurring on each of the three Patterson projections, selection of A as the Ca-Ca interaction was confirmed. Peak B was later found to be the result of three "non-Harker" superpositions, i.e. two Ca-O vectors, one with $v = \frac{1}{2}$ and one with $v \approx \frac{1}{2}$, and one O-O vector with $v \approx \frac{1}{2}$.

The x,y,z coordinates for calcium given in Table 1 were established from calculations of peak maxima on the Harker section and on each Patterson projection. Structure factors based on the calcium contribution only were calculated for the three zones and gave the following residuals: R(hk0), 0.55; R(h0ℓ), 0.50; R(0kℓ), 0.54; (Appendix III). The first electron-density projections were prepared using as coefficients those terms which could reasonably be considered fixed in sign according to these structure factors (Appendices II and III). The series for $\rho_y(x,z)$ included about two-thirds of the possible 149 terms. However, the calculations for each of the other two projections included only about one-third of the possible 180 terms, since many hk0 and 0kℓ structure factors received only a small contribution from the calcium atom as a result of its having an x-coordinate of nearly zero and a y-coordinate of about one-eighth.

Application of a superposition method (Appendix II) appeared to be a useful supplementary approach to the problem of locating oxygen atoms. Accordingly the minimum-function technique, described by Buerger (1951), was applied in turn to

Table 1. Calcium coordinates from Patterson functions

Parameter	Harker Section	$P_w(u,v)$	$P_v(u,w)$	$P_u(v,w)$	Ave.
x	0.022	0.021	0.023	–	0.022
y	–	0.130	–	0.130	0.130
z	0.161	–	0.160	0.156	0.159

each Patterson projection, the known Ca-Ca inversion peaks being used as a basis for a first superposition, and the glide plane symmetry used for a second superposition to produce the three approximate electron-density maps. Each of these maps was similar in detail to the corresponding first electron-density projection described above. Study of all the maps showed that there must be many overlapping atoms in the structure viewed along [100], so principal attention was directed to the other two projections.

The coordinates for selected peaks from each projection were assigned the oxygen scattering factor and their total contribution was added to the calcium contribution for calculation of both hk0 and h0ℓ structure factors (S.F.). The residuals for both zones remained persistently higher than those obtained for calcium alone. Examination of individual atomic contributions to the $F_{h0\ell}$ revealed that subtraction of the contribution of one "atom" led ultimately to an R of 0.34 for a set of S.F. containing calcium and twelve oxygens. The $\rho_y(x,z)$ based on that set of S.F. included 120 terms and showed no trace of the original false peak. Consideration of the oxygen coordination that could reasonably be expected about the calcium atom led to selection of x- and y-coordinates for six oxygen atoms; the calculated F_{hk0} based on these six oxygens and the calcium gave an R of 0.45. The ensuing $\rho_z(x,y)$ contained 128 terms, and study of this analysis, taken together with the last $\rho_y(x,z)$ and a ball model, revealed the structure.

The atomic coordinates assigned for the next S.F. calculation are listed in Table 2, column 1. The oxygen O_{12} of one water molecule was omitted from this calculation but its position was immediately evident on the next electron-density projections, which gave coordinates for all atoms as shown in Table 2, column 2.

A final set of electron-density projections was then prepared, each series containing 99% of all possible terms. Any omitted term had a very small $|F_o|$. The final $\rho_z(x,y)$ and $\rho_y(x,z)$, which are on an absolute scale, are shown in Figs. 2 and 3 and the atomic coordinates taken from all three projections are given in Table 2, column 3. Difference syntheses, $D_z(x,y)$ and $D_y(x,z)$, were calculated (Appendix IV) and the indicated shifts in atomic positions yielded the coordinates listed in Table 2, column 4. Comparison of F_o with the F_c obtained from the S.F. based on this last set of coordinates is shown in Table 3; the R value for each of the three zones is 0.15. Further refinement of the structure from the three-dimensional data is planned, and a detailed analysis of the accuracy of the structure parameters and of the bond distances has therefore been postponed. For the colemanite structure (Christ, Clark and Evans, 1958) standard errors in bond distances were calculated following least-squares refinement of atomic coordinates. Because the inyoite structure is directly comparable to colemanite and both structures are at a similar stage of refinement, standard errors for bond distances in inyoite may reasonably be expected to be the same as for colemanite. On this basis the limits assigned

Table 2. Refinement of atomic coordinates (cycles)

Atom	Parameter	Stage of refinement 1	2	3	4
Ca	x	0.020	0.020	0.020	0.022
	y	.131	.130	.130	.129
	z	.156	.158	.160	.160
O_1*	x	.044	.043	.041	.043
	y	.200	.204	.205	.208
	z	.915	.919	.913	.912
O_2*	x	.137	.140	.138	.137
	y	.483	.482	.483	.486
	z	.782	.786	.786	.787
O_3	x	.172	.180	.175	.174
	y	.134	.133	.131	.131
	z	.752	.750	.750	.752
O_4†	x	.041	.040	.040	.040
	y	.331	.334	.334	.334
	z	.217	.212	.216	.216
O_5	x	.167	.168	.166	.164
	y	.467	.481	.490	.490
	z	.083	.080	.081	.081
O_6*	x	.127	.128	.125	.123
	y	.603	.600	.600	.601
	z	.292	.290	.291	.290
O_7	x	.140	.136	.138	.139
	y	.032	.032	.032	.032
	z	.991	.980	.980	.982
O_8†	x	.066	.061	.057	.057
	y	.863	.856	.854	.851
	z	.613	.631	.612	.615
O_9†	x	.234	.238	.236	.236
	y	.652	.652	.650	.650
	z	.649	.632	.641	.644

O_{10}*	x	.226	.221	.221	.220
	y	.854	.848	.848	.848
	z	.011	.012	.010	.010
O_{11}*	x	.044	.044	.048	.048
	y	.936	.938	.938	.940
	z	.299	.295	.295	.296
O_{12}†	x	—	.186	.188	.188
	y	—	.332	.331	.331
	z	—	.579	.586	.586
B_1	x	0.100	0.095	0.077	.073
	y	.100	.105	.104	.108
	z	.817	.830	.831	.835
B_2	x	.228	.229	.232	.232
	y	.463	.463	.467	.467
	z	.975	.980	.980	.976
B_3	x	.192	.200	.206	.206
	y	.577	.580	.580	.578
	z	.175	.197	.213	.211

R	hk0	0.32	0.21	0.17	0.15
	h0ℓ	.32	.24	.17	.15
	0kℓ	.33	.20	.16	.14
B	hk0	0.9	1.15	1.09	0.94
	h0ℓ	1.2	1.36	1.30	1.07
	0kℓ	1.2	1.42	1.20	1.09
k	hk0	3.1	3.0	3.1	3.2
	h0ℓ	2.3	2.3	2.3	2.5
	0kℓ	2.8	2.7	2.9	2.9

$R = \Sigma|\Delta F| / \Sigma|F_o|$, ΔF omitted if $F_o = 0$

B = average isotropic temperature factor ($Å^2$)

k = scaling factor (see text)

---

*Hydroxyl oxygen

†Water oxygen

Table 3

Comparison of observed and calculated structure factors for the three zones: hk0, h0ℓ, 0kℓ. Calculated $F_{hk\ell}$ are based on the atomic coordinates of Table 2, column 4.

hk0	F_o	F_c	hk0	F_o	F_c
0 2 0	49	53	2 19 0	7	12-
0 4 0	119	111-	2 20 0	7	6-
0 6 0	103	91	2 21 0		6
0 8 0	56	52	3 1 0	109	92
0 10 0	30	25-	3 2 0	18	13-
0 12 0	21	14-	3 3 0	12	13-
0 14 0	11	16	3 4 0		1-
0 16 0		1-	3 5 0		2-
0 18 0		4-	3 6 0	7	7
0 20 0	7	5-	3 7 0	17	17
1 1 0	53	63	3 8 0	22	21
1 2 0	33	28-	3 9 0	25	29
1 3 0	70	68-	3 10 0	30	29-
1 4 0	32	28-	3 11 0		1
1 5 0	38	44-	3 12 0	17	22-
1 6 0	42	35	3 13 0		3
1 7 0	11	11	3 14 0	9	10
1 8 0	42	38	3 15 0	18	20
1 9 0	15	14	3 16 0		8
1 10 0	15	13-	3 17 0	11	8
1 11 0	55	57-	3 18 0	9	4
1 12 0		4	3 19 0		2-
1 13 0	22	20-	3 20 0		4
1 14 0	16	17	3 21 0		2-
1 15 0	26	30	4 0 0	54	42
1 16 0		3-	4 1 0	24	18-
1 17 0		2-	4 2 0	67	63-
1 18 0	9	4	4 3 0	12	16
1 19 0		11-	4 4 0	68	73-
1 20 0		11	4 5 0	30	26
1 21 0		1-	4 6 0	16	16
2 0 0	35	26	4 7 0	31	28
2 1 0	44	36-	4 8 0		2
2 2 0	38	32-	4 9 0	12	13
2 3 0	7	4	4 10 0	37	37-
2 4 0	37	36-	4 11 0		7-
2 5 0		1	4 12 0	17	17
2 6 0	26	26-	4 13 0	12	10
2 7 0	33	32-	4 14 0	16	19
2 8 0	12	11	4 15 0		0
2 9 0	29	33-	4 16 0	10	7
2 10 0	6	5	4 17 0		2
2 11 0	27	32-	4 18 0		6-
2 12 0	25	32-	4 19 0		3
2 13 0	6	8-	4 20 0		6-
2 14 0		5	4 21 0		3
2 15 0		0	5 1 0	17	16
2 16 0	17	21	5 2 0	8	12
2 17 0	11	11-	5 3 0	28	29-
2 18 0		4	5 4 0	20	22

hk0	F_o	F_c
5 5 0	32	34-
5 6 0	15	12
5 7 0	25	22
5 8 0	17	20
5 9 0	20	28
5 10 0	20	22-
5 11 0	22	24-
5 12 0		10-
5 13 0	7	10-
5 14 0	7	8
5 15 0	19	21
5 16 0	15	15-
5 17 0		2
5 18 0	10	14-
5 19 0	7	7-
5 20 0		5-
6 0 0	38	37
6 1 0	32	32-
6 2 0	17	17
6 3 0	9	7
6 4 0		0
6 5 0	33	36
6 6 0	14	16
6 7 0	28	28
6 8 0	24	27
6 9 0	6	7
6 10 0		8
6 11 0	24	24-
6 12 0	9	10-
6 13 0	8	4
6 14 0	7	4
6 15 0	13	18
6 16 0	17	20
6 17 0		3
6 18 0		3-
6 19 0		6-
6 20 0	12	16-
7 1 0		3-
7 2 0	9	2-
7 3 0	11	9-
7 4 0		0
7 5 0	10	10-
7 6 0	22	19
7 7 0		1
7 8 0	9	15
7 9 0	8	9-
7 10 0	32	38-
7 11 0	15	17-
7 12 0	6	3
7 13 0	11	12-

hk0	F_o	F_c
7 14 0	25	28
7 15 0		2
7 16 0	15	15-
8 0 0		4-
8 1 0	50	50-
8 2 0	22	20
8 3 0	20	20-
8 4 0		6
8 5 0	34	36
8 6 0		2-
8 7 0		0
8 8 0	18	20
8 9 0	28	27-
8 10 0		4
8 11 0	8	9-
8 12 0	10	12-
8 13 0	12	10
8 14 0	7	7-
8 15 0	10	11-
8 16 0		3-
9 1 0	10	14-
9 2 0	29	28-
9 3 0		4
9 4 0	16	16
9 5 0	6	14
9 6 0	25	21
9 7 0	18	18
9 8 0		6-
9 9 0		0
9 10 0	16	18-
9 11 0		8
9 12 0		6
9 13 0	7	4
9 14 0	11	13
9 15 0		1-
9 16 0	4	2-
10 0 0	27	29-
10 1 0		2-
10 2 0	14	10-
10 3 0		0
10 4 0	20	14-
10 5 0		3-
10 6 0	10	15-
10 7 0		5-
10 8 0		0
10 9 0	14	17-
10 10 0	4	4
10 11 0	11	14-
10 12 0		3
10 13 0	10	13

hk0	F_o	F_c
10 14 0		5-
10 15 0		5
10 16 0	6	6
11 1 0		1
11 2 0	23	19-
11 3 0		1
11 4 0	13	10-
11 5 0	10	10-
11 6 0	10	12
11 7 0	10	12
11 8 0		3
11 9 0	8	11
11 10 0	14	16-
11 11 0		4
11 12 0		1
11 13 0		2-
11 14 0	12	9
11 15 0		3-
11 16 0	8	10-
12 0 0	24	21-
12 1 0	26	28-
12 2 0		2
12 3 0	12	11-
12 4 0		3
12 5 0	28	40
12 6 0		3
12 7 0	9	8
12 8 0	11	14
12 9 0	14	15-
12 10 0		2
12 11 0	6	14
12 12 0		3-
12 13 0	15	20
12 14 0		1-
12 15 0		1
13 1 0		2-
13 2 0	24	24-
13 3 0	8	10-
13 4 0	10	10
13 5 0		8-
13 6 0	23	26
13 7 0		0
13 8 0	8	15-
13 9 0		6-
13 10 0	8	14-
13 11 0	8	12
13 12 0	9	16
13 13 0		1
13 14 0	10	12
14 0 0		7-

hk0	F_o	F_c
14 1 0	12	9-
14 2 0		12
14 3 0	22	22-
14 4 0	8	10
14 5 0		2
14 6 0		4-
14 7 0	10	14
14 8 0		0
14 9 0	8	10-
14 10 0		2
14 11 0		8-
14 12 0	9	4
15 1 0		0
15 2 0	12	14-
15 3 0		7
15 4 0	7	2-
15 5 0	8	8
15 6 0		7
15 7 0		4
15 8 0		7-
15 9 0		8-
15 10 0		1-
15 11 0		1
16 0 0		4-
16 1 0		6-
16 2 0		1
16 3 0	7	12-
16 4 0		1
16 5 0		6
16 6 0		4-
16 7 0		4
16 8 0		5-
17 1 0		6-
17 2 0	15	15-
17 3 0		3
17 4 0		6-
17 5 0		2

h0ℓ	F_o	F_c
0 0 1	73	110
0 0 2	73	63-
0 0 3	10	16
0 0 4		3
0 0 5	46	50
0 0 6	26	17
0 0 7	16	14
0 0 8		1
0 0 9	11	12-
0 0 10	6	8
0 0 11	6	8
0 0 12	10	11
0 0 13	14	19
2 0 0	27	26
2 0 1	26	20
2 0 2	88	82-
2 0 3	62	55-
2 0 4	69	68-
2 0 5	7	7-
2 0 6	44	45
2 0 7	8	3
2 0 8	13	16-
2 0 9	17	17-
2 0 10		3
2 0 11		0
2 0 12	8	6
2 0 13	19	23
2 0 1-	11	8
2 0 2-	57	56-
2 0 3-	136	122-
2 0 4-	22	16-
2 0 5-	36	49-
2 0 6-	16	15-
2 0 7-	36	32
2 0 8-	8	16-
2 0 9-	41	47-
2 0 10-	21	19-
2 0 11-		0
2 0 12-		0
2 0 13-	11	8
2 0 14-		0
4 0 0	42	42
4 0 1	42	37-
4 0 2	19	14
4 0 3	20	20
4 0 4	14	10-
4 0 5	13	14
4 0 6	32	36
4 0 7		2-
4 0 8	14	14-

h0ℓ	F_o	F_c
4 0 9	16	15-
4 0 10	17	21-
4 0 11		7
4 0 12	11	10
4 0 1-	63	70
4 0 2-	26	19-
4 0 3-	106	98-
4 0 4-	97	89-
4 0 5-	26	26
4 0 6-	36	31
4 0 7-	27	23
4 0 8-	24	28
4 0 9-		0
4 0 10-		7-
4 0 11-	11	4-
4 0 12-		8
4 0 13-		6
4 0 14-		0
6 0 0	30	36
6 0 1		1-
6 0 2	49	56-
6 0 3	5	0
6 0 4	22	28
6 0 5	13	8
6 0 6	9	16-
6 0 7	15	18-
6 0 8	9	9-
6 0 9	6	8-
6 0 10		12-
6 0 11		5-
6 0 1-	56	56
6 0 2-	39	43
6 0 3-	98	102-
6 0 4-	39	39-
6 0 5-	14	7-
6 0 6-		4-
6 0 7-	51	48
6 0 8-	6	3-
6 0 9-		1
6 0 10-		7
6 0 11-		3-
6 0 12-	8	10
6 0 13-	7	4
6 0 14-	11	10
6 0 15-		6
8 0 0		4-
8 0 1	13	8-
8 0 2	17	16-
8 0 3	7	3-
8 0 4	14	16

hOℓ	F_o	F_c
8 0 5	29	24
8 0 6	27	30
8 0 7	7	7-
8 0 8	12	10-
8 0 9		0
8 0 1-	33	48
8 0 2-	21	20
8 0 3-	17	11
8 0 4-		4-
8 0 5-	36	38-
8 0 6-	28	26
8 0 7-	40	35
8 0 8-	21	22
8 0 9-		4
8 0 10-	27	28-
8 0 11-	22	15-
8 0 12-	14	14-
8 0 13-		4-
8 0 14-	18	16
8 0 15-		3
10 0 0	21	28-
10 0 1	36	39-
10 0 2	16	10-
10 0 3		2-
10 0 4	17	22
10 0 5	22	16
10 0 6	12	12
10 0 7		4
10 0 8	16	20-
10 0 1-	25	27
10 0 2-	17	15
10 0 3-	33	35-
10 0 4-	33	37-
10 0 5-	14	21-
10 0 6-	13	10-
10 0 7-	27	27
10 0 8-	32	36
10 0 9-		1
10 0 10-	25	21-
10 0 11-	22	24-
10 0 12-	7	7-
10 0 13-		0
10 0 14-	7	11
12 0 0	19	20-
12 0 1	21	26-
12 0 2	13	10-
12 0 3	8	6-
12 0 4		2
12 0 5	11	13
12 0 6	6	8-

hOℓ	F_o	F_c
12 0 1-	21	20
12 0 2-	28	30
12 0 3-		1
12 0 4-	26	30-
12 0 5-	32	36-
12 0 6-	5	10
12 0 7-	14	17
12 0 8-	23	20
12 0 9-	8	7
12 0 10-	32	35-
12 0 11-		2-
12 0 12-	14	14
12 0 13-		3-
12 0 14-		6
14 0 0		6-
14 0 1		0
14 0 2	9	7-
14 0 3	8	10-
14 0 4	16	17
14 0 1-	8	11
14 0 2-	31	29
14 0 3-	22	24
14 0 4-	6	9-
14 0 5-		1
14 0 6-	11	17
14 0 7-		1
14 0 8-	8	16
14 0 9-	7	5
14 0 10-		3-
14 0 11-	12	14-
14 0 12-	15	16-
14 0 13-	9	13
16 0 0		4-
16 0 1	12	19-
16 0 2	7	5-
16 0 1-		9-
16 0 2-		1
16 0 3-	16	16
16 0 4-		7-
16 0 5-	14	13-
16 0 6-	9	9-
16 0 7-		0
16 0 8-	7	5
16 0 9-	16	9
16 0 10-		3-
16 0 11-	15	19-
16 0 12-	11	11-

Okl	F_o	F_c
0 2 0	44	53
0 4 0	108	110-
0 6 0	93	90
0 8 0	50	51
0 10 0	27	24-
0 12 0	19	13-
0 14 0	10	15
0 16 0		1-
0 18 0		3-
0 20 0	6	5-
0 0 1	85	110
0 1 1	7	4-
0 2 1	65	54
0 3 1	34	35
0 4 1	35	39
0 5 1	84	84
0 6 1	16	17
0 7 1		2-
0 8 1	31	30
0 9 1	32	39-
0 10 1	8	12
0 11 1	10	12
0 12 1	25	26-
0 13 1	11	15
0 14 1	5	2
0 15 1		0
0 16 1		2
0 17 1	10	6-
0 18 1	8	8-
0 19 1		2
0 20 1	6	7-
0 21 1	9	8
0 0 2	85	63-
0 1 2	8	4-
0 2 2	21	14-
0 3 2	44	36-
0 4 2	73	70
0 5 2	20	16
0 6 2	33	28
0 7 2	20	16
0 8 2	21	20-
0 9 2	16	10-
0 10 2	4	7-
0 11 2	5	5-
0 12 2	3	0
0 13 2	8	4
0 14 2	5	8-
0 15 2	15	20
0 16 2	17	20-
0 17 2	14	13-
0 18 2	6	4-
0 19 2	9	15-
0 20 2	6	5
0 21 2	11	11
0 0 3	12	16
0 1 3	7	3-
0 2 3	20	17-
0 3 3	70	66-
0 4 3	30	24
0 5 3		2-
0 6 3	10	8
0 7 3	25	29
0 8 3	35	34-
0 9 3	22	22-
0 10 3	19	23-
0 11 3		4-
0 12 3	14	14
0 13 3	6	7
0 14 3	8	4-
0 15 3		8-
0 16 3	23	27-
0 17 3	12	17-
0 18 3		0
0 19 3		1-
2 20 3	16	16
0 21 3		4-
0 0 4		3
0 1 4	47	44
0 2 4	44	40
0 3 4	24	27
0 4 4	27	27
0 5 4	10	12-
0 6 4	10	10-
0 7 4	8	11-
0 8 4	12	17-
0 9 4	11	12
0 10 4	4	2-
0 11 4	10	7
0 12 4	6	8
0 13 4	22	26-
0 14 4	10	13-
0 15 4	12	11-
0 16 4	9	9-
0 17 4		0
0 18 4		1-
0 19 4		5-
0 20 4		2-
0 0 5	53	50
0 1 5	60	60
0 2 5	4	3-

Okℓ	F_o	F_c
0 3 5	40	40
0 4 5	28	30–
0 5 5	38	38–
0 6 5	41	44
0 7 5	4	5–
0 8 5	7	12
0 9 5	38	38
0 10 5	21	28–
0 11 5	9	7
0 12 5	8	8
0 13 5	21	23–
0 14 5		3–
0 15 5		3
0 16 5	7	10–
0 17 5	13	13
0 18 5		7–
0 19 5		4–
0 20 5	10	9–
0 0 6	30	17
0 1 6	14	17–
0 2 6	12	11
0 3 6	5	1–
0 4 6	35	35–
0 5 6	13	18
0 6 6		8–
0 7 6		3
0 8 6	19	22
0 9 6	14	10
0 10 6	16	18–
0 11 6	14	17
0 12 6	17	21–
0 13 6		2
0 14 6		4–
0 15 6		2
0 16 6		3
0 17 6	13	12
0 18 6	8	8–
0 19 6		2
0 0 7	18	14
0 1 7	15	12–
0 2 7		3
0 3 7	5	5
0 4 7	30	31–
0 5 7	26	23
0 6 7	12	16–
0 7 7	18	16
0 8 7	9	8
0 9 7		2–
0 10 7	9	10–
0 11 7	4	6–

Okℓ	F_o	F_c
0 12 7	18	20–
0 13 7	16	16
0 14 7	11	13–
0 15 7	7	7
0 16 7	5	6
0 17 7	9	11–
0 18 7		0
0 0 8		1
0 1 8	4	1–
0 2 8	9	7–
0 3 8		4
0 4 8	8	10–
0 5 8	11	8
0 6 8	9	12
0 7 8	16	22
0 8 8	5	5
0 9 8	5	5–
0 10 8	10	17–
0 11 8	8	13–
0 12 8	5	4–
0 13 8	20	24
0 14 8		3
0 15 8		1–
0 16 8	7	8–
0 17 8	16	20–
0 0 9	13	12–
0 1 9	15	15–
0 2 9		2
0 3 9		3–
0 4 9	24	26
0 5 9	7	8
0 6 9	8	10
0 7 9	5	6
0 8 9	16	18–
0 9 9	7	11
0 10 9	5	1–
0 11 9	5	6
0 12 9	12	15
0 13 9	8	7
0 14 9		0
0 15 9		0
0 16 9	11	11–
0 0 10	7	8
0 1 10	10	10
0 2 10	7	7
0 3 10	10	13
0 4 10	20	19
0 5 10	5	6–
0 6 10		2
0 7 10	8	9

Okℓ			F_o	F_c
0	8	10	19	20-
0	9	10	16	22
0	10	10		4
0	11	10		2
0	12	10	14	16
0	13	10		1-
0	14	10		2-
0	0	11	7	7
0	1	11	11	9
0	2	11		1-
0	3	11	16	19
0	4	11		1-
0	5	11		7
0	6	11		0
0	7	11		0
0	8	11		6
0	9	11	12	12
0	10	11		2
0	11	11	8	8
0	12	11		6-
0	13	11	8	4-
0	0	12	11	11
0	1	12	7	8
0	2	12	7	7-
0	3	12	5	5
0	4	12	10	10-
0	5	12		3-
0	6	12		8
0	7	12		3
0	8	12	11	14
0	9	12	7	8
0	10	12		1
0	0	13	16	18
0	1	13		5
0	2	13		2
0	3	13		5-
0	4	13	9	9-
0	5	13		6-
0	6	13		3
0	7	13		9

to bond distances in inyoite are as follows: Ca-O, ±0.02; O-O, ±0.03; B-O, ±0.04 (Å).

Discussion of Structure

The crystal structure of inyoite contains isolated polyions, $[B_3O_3(OH)_5]^{-2}$, one of which is illustrated in Fig. 2 as it appears on $\rho_z(x,y)$. Single polyions are connected to one another (Fig. 4) to form continuous polyion-calcium-water columns parallel to [100]. The polyions within one column are held together principally by bonding from calcium ions to oxygens and hydroxyls of adjacent polyions and to oxygens of water molecules. Some hydrogen bonds also link adjacent polyions to one another and to water molecules. Each calcium ion is coordinated by eight oxygens, three from water molecules and five from polyions within one column. This coordination is shown in Fig. 3 as it appears on $p_y(x,z)$. Two cleavages have been observed, one (Schaller, 1916) parallel to (001), the other (Bokiĭ, 1937) parallel to (010). Cleavage is easily produced in both directions, but the cleavage planes are not perfect. They lie between the columns and the bonds they break can be seen on Fig. 5, which shows the structure viewed along [100]. The (001) cleavage breaks only three hydrogen bonds, while the (010) cleavage breaks two hydrogen bonds and one Ca-H_2O bond.

The $[B_3O_3(OH)_5]^{-2}$ polyion is formed by two BO_4 tetrahedra sharing a corner and linked by a BO_3 triangle, which has one corner in common with each of the two tetrahedra. It was found

first in meyerhofferite (Christ and Clark, 1956) and later in synthetic $2CaO.3B_2O_3.9H_2O$ (Clark and Christ, 1957). All the members of the series are listed in Table 4, together with their chemical formulas as determined from the crystal structures. Existence of the $[B_3O_3(OH)_5]^{-2}$ polyion was postulated from chemical evidence alone by Ingri, Lagerström, Frydman and Sillén (1957). The infinite boron-oxygen chains of colemanite may formally be derived from the isolated polyions by the condensation and dehydration reaction (Christ, Clark and Evans, 1958),

$$n[B_3O_3(OH)_5]^{-2} = [B_3O_4(OH)_3]_n^{-2n} + nH_2O.$$

The close structural relationship among the members of the series explains the occurrence in nature of colemanite and meyerhofferite pseudomorphs after inyoite (Palache, Berman and Frondel, 1951).

Bond lengths and angles as found for inyoite within the polyion are given in Tables 5 and 6, and the average values for boron-oxygen distances are compared in Table 7 with corresponding average values for some other borates. Individual variations within either tetrahedra or triangle of inyoite are not considered significant at present, but there is ample evidence from several borate structure determinations that a real difference exists between the B-O distance for tetrahedrally-coordinated boron and for triangularly-coordinated boron. This point has previously been discussed in detail (Christ, Clark and Evans, 1958).

Calcium-oxygen distances and some O-Ca-O angles are given in Table 8. Four of the eight oxygens coordinating calcium

Table 4. Series, $2CaO.3B_2O_3.xH_2O$

x	Mineral	Formula
5	Colemanite	$CaB_3O_4(OH)_3.H_2O$
7	Meyerhofferite	$CaB_3O_3(OH)_5.H_2O$
9	(Synthetic)	$CaB_3O_3(OH)_5.2H_2O$
13	Inyoite	$CaB_3O_3(OH)_5.4H_2O$

Table 5. Boron-oxygen bond lengths and bond angles for inyoite

(See Fig. 2)

B-O bonds (Å)		Bond angles (°)	
Triangle around B_3			
B_3-O_5	1.46	O_5-B_3-O_6	117.5
B_3-O_6*	1.33	O_6-B_3-O_3	123.0
B_3-O_3	1.34	O_5-B_3-O_3	119.5
Average =	1.38	Σ =	360.0
Tetrahedron around B_1			
B_1-O_1*	1.46	O_1-B_1-O_7	105.0
B_1-O_7	1.47	O_1-B_1-O_3	111.9
B_1-O_3	1.52	O_1-B_1-O_{11}	112.6
B_1-O_{11}*	1.43	O_7-B_1-O_3	108.3
Average =	1.47	O_7-B_1-O_{11}	111.5
		O_3-B_1-O_{11}	107.5
		Average =	109.5
Tetrahedron around B_2			
B_2-O_5	1.38	O_5-B_2-O_2	110.0
B_2-O_2*	1.51	O_5-B_2-O_7	114.5
B_2-O_7	1.49	O_5-B_2-O_{10}	113.0
B_2-O_{10}*	1.51	O_2-B_2-O_7	109.0
Average =	1.47	O_2-B_2-O_{10}	106.6
		O_7-B_2-O_{10}	103.4
		Average =	109.4

*Hydroxyl oxygens

Table 6. Oxygen-oxygen distances for inyoite within the $[B_3O_3(OH)_5]^{-2}$ polyion

(See Fig. 2)

	O-O (Å)				
Triangle around B_3		Tetrahedron around B_1		Tetrahedron around B_2	
O_5-O_6*	2.39	O_7-O_3	2.43	O_7-O_5	2.41
O_3-O_6*	2.35	O_7-O_1*	2.32	O_7-O_2*	2.44
O_3-O_5	2.42	O_7-O_{11}*	2.40	O_7-O_{10}*	2.38
Average =	2.39	O_3-O_1*	2.48	O_5-O_{10}*	2.41
		O_3-O_{11}*	2.38	O_5-O_2*	2.37
		O_1*-O_{11}*	2.41	O_2*-O_{10}*	2.42
		Average =	2.40	Average =	2.40

*Hydroxyl oxygen

Table 7. Comparison of average B-O bond lengths for inyoite and other borates

Compound	Average B-O distance (Å) Triangle	Tetrahedra	Reference
Colemanite	1.37	1.48	Christ, Clark and Evans, 1958
Meyerhofferite	1.38	1.49	Christ and Clark, 1956
$2CaO.3B_2O_3.9H_2O$	1.37	1.47	Clark and Christ, 1957
Borax	1.36	1.48	Morimoto, 1956
Metaboric acid	1.36	1.46	Zachariasen, 1952
Inyoite	1.38	1.47	Present study

Table 8. Calcium-oxygen bond lengths and angles for inyoite

(See Fig. 3)

Ca-O bonds (Å)		O-Ca-O angles (°)	
$Ca-O_1$*	2.38	O_1-Ca-O_9	95.8
$Ca-O_{10}$*	2.40	O_9-Ca-O_8	94.0
$Ca-O_8'$†	2.37	O_8-Ca-O_{10}	81.0
$Ca-O_9$†	2.44	O_1-Ca-O_{10}	89.1
Average of 4 =	2.40	Σ =	359.9
$Ca-O_7$	2.59		
$Ca-O_7'$	2.54		
$Ca-O_{11}$*	2.51		
$Ca-O_4$†	2.51		
Average of 4 =	2.54		
Average of 8 =	2.47		

*Hydroxyl oxygen

†Water oxygen

are contained with calcium in a plane nearly parallel to (010) and are arranged in an almost square array about calcium at an average distance of 2.40 Å. The other four coordinating oxygens are located irregularly about calcium at an average 2.54 Å distance. The closest Ca-Ca approach is 4.0 Å.

Hydrogen bonds have been identified on the basis of length, distances of 2.7 to 2.9 Å being considered indicative when at least one of the oxygens involved had been identified as belonging to hydroxyl ion or water molecule. Consideration of these bonds permits a tentative count of hydrogens and identification of their associated oxygens. The bond distances and contributor oxygens are given in Table 9, while the various bonds have been illustrated in Figs. 4 and 5. Of the thirteen hydrogens in each formula unit, only two presumably do not enter into hydrogen bonds. One of these two is associated with O_8 in a water molecule (although this one may be participating in a long bond listed in Table 9), while the other is associated with either O_1 or O_{10} in hydroxyl ion. No evidence was found for any disordering of hydrogens such as was discovered in colemanite (Christ, Clark and Evans, 1958), but the possibility cannot yet be entirely eliminated. The further refinement of the structure should resolve this question.

Table 9. Oxygen-oxygen distances for postulated hydrogen bonds in inyoite

(See Figs. 4 and 5)

O-O distance (Å)		Contributor Oxygen
O_2*-O_4'†	2.87	O_4'†
O_5-O_4''†	2.79	O_4''†
O_{11}*-O_8†	2.85	O_8†
O_2*-O_9†	2.74	O_9†
O_6'*-O_9†	2.78	O_9†
O_3-O_{12}†	2.82	O_{12}†
O_4†-O_{12}†	2.86	O_{12}†
O_2*-O_{12}''†	2.72	O_2*
O_{11}*-O_{12}''†	2.88	O_{11}*
O_6*-O_2*	2.78	O_6*
O_{10}'*-O_1*	2.88	either
(O_{11}'*-O_8†	2.97	O_8†)

*Hydroxyl oxygen

†Water oxygen

Figure 1

Sharpened Harker section, P(u, $\frac{1}{2}$, w). Contours at arbitrary levels, the dashed line at the lowest level and others at intervals of 200, except around A and B where the intervals become 400. A designates the Ca-Ca Harker peak; B is a peak caused by superposition of three "non-Harker" interactions.

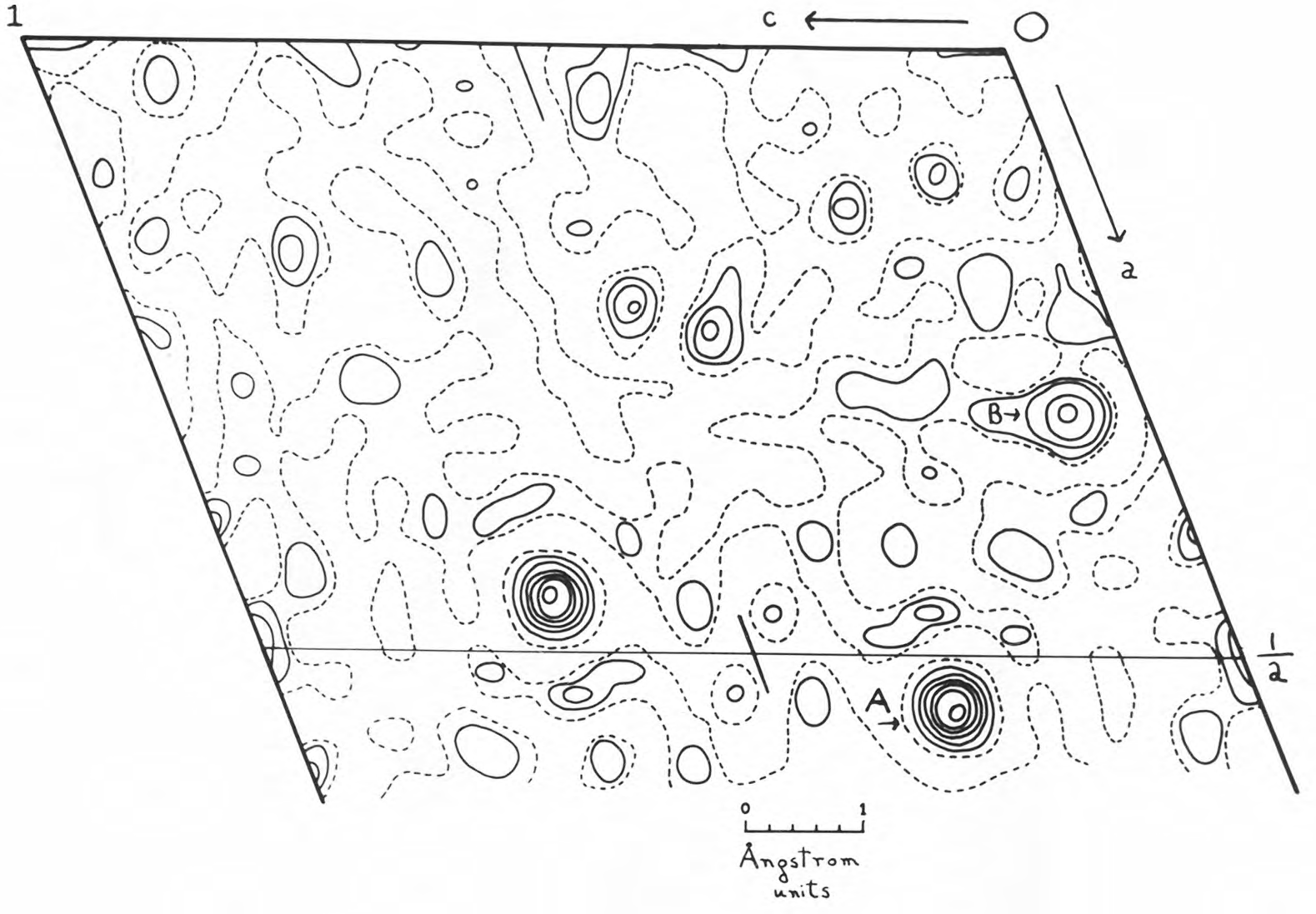

Figure 1

Figure 2

Final $\rho_z(x,y)$. Contours at intervals of $4e/\mathring{A}^2$ except around Ca where intervals become $10e/\mathring{A}^2$ after the $20e/\mathring{A}^2$ contour. Dashed contour at $4e/\mathring{A}^2$. Orientation of the $[B_3O_3(OH)_5]^{-2}$ polyion is shown. Atomic sites are marked: open circles for oxygens or hydroxyl oxygens; spoked circles for water oxygens. Tables 5 and 6 list bond distances and angles within the polyion.

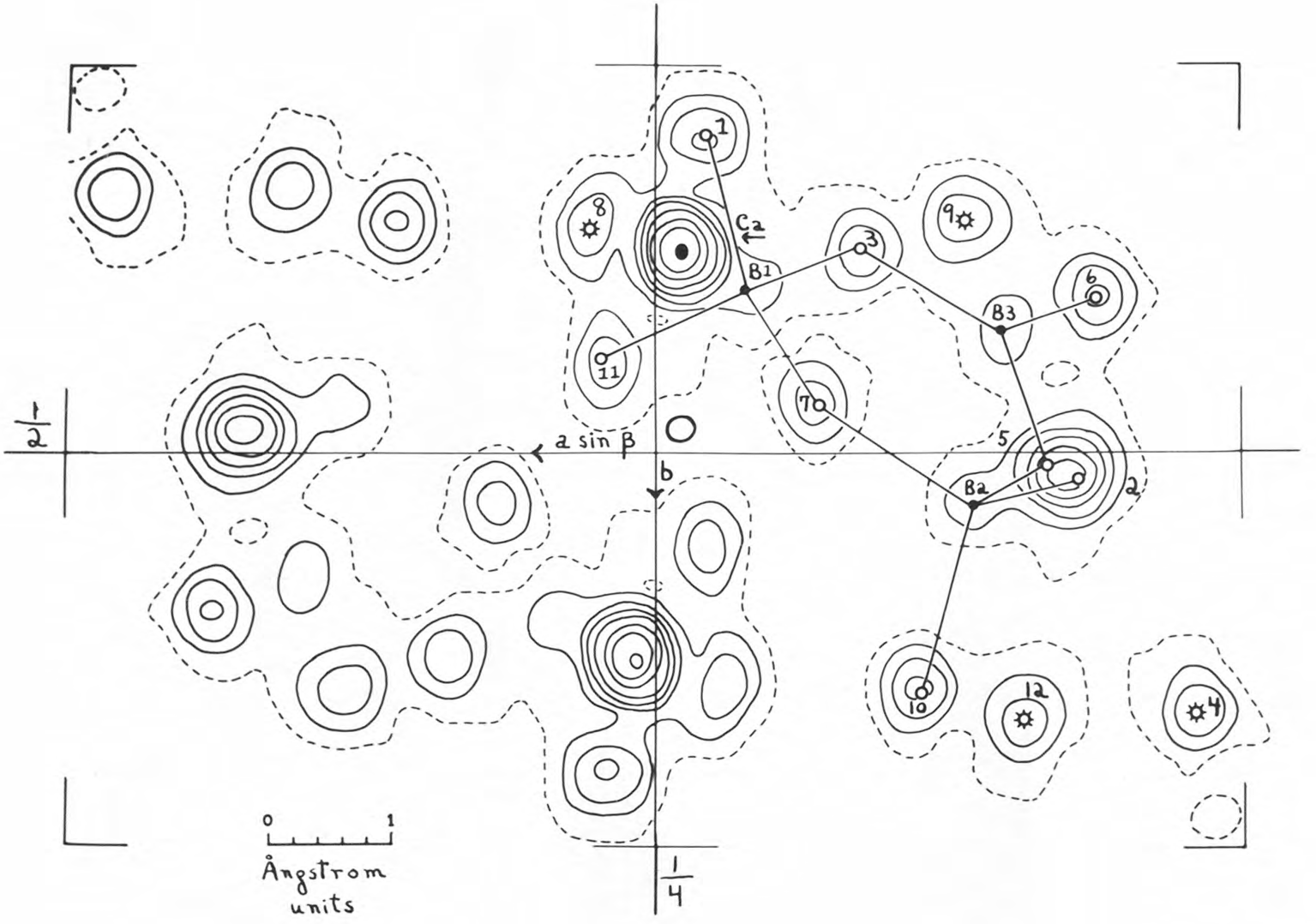

Figure 2

Figure 3

Final $\rho_y(x,z)$. Contours at intervals of $4e/\mathring{A}^2$ except around Ca where intervals become $10e/\mathring{A}^2$ after the $20e/\mathring{A}^2$ contour. Dashed contour at $4e/\mathring{A}^2$. Oxygen coordination around one Ca ion is shown; open circles are at sites of oxygens or hydroxyl oxygens, and spoked circles are at sites of water oxygens. Table 8 lists Ca-O bond distances.

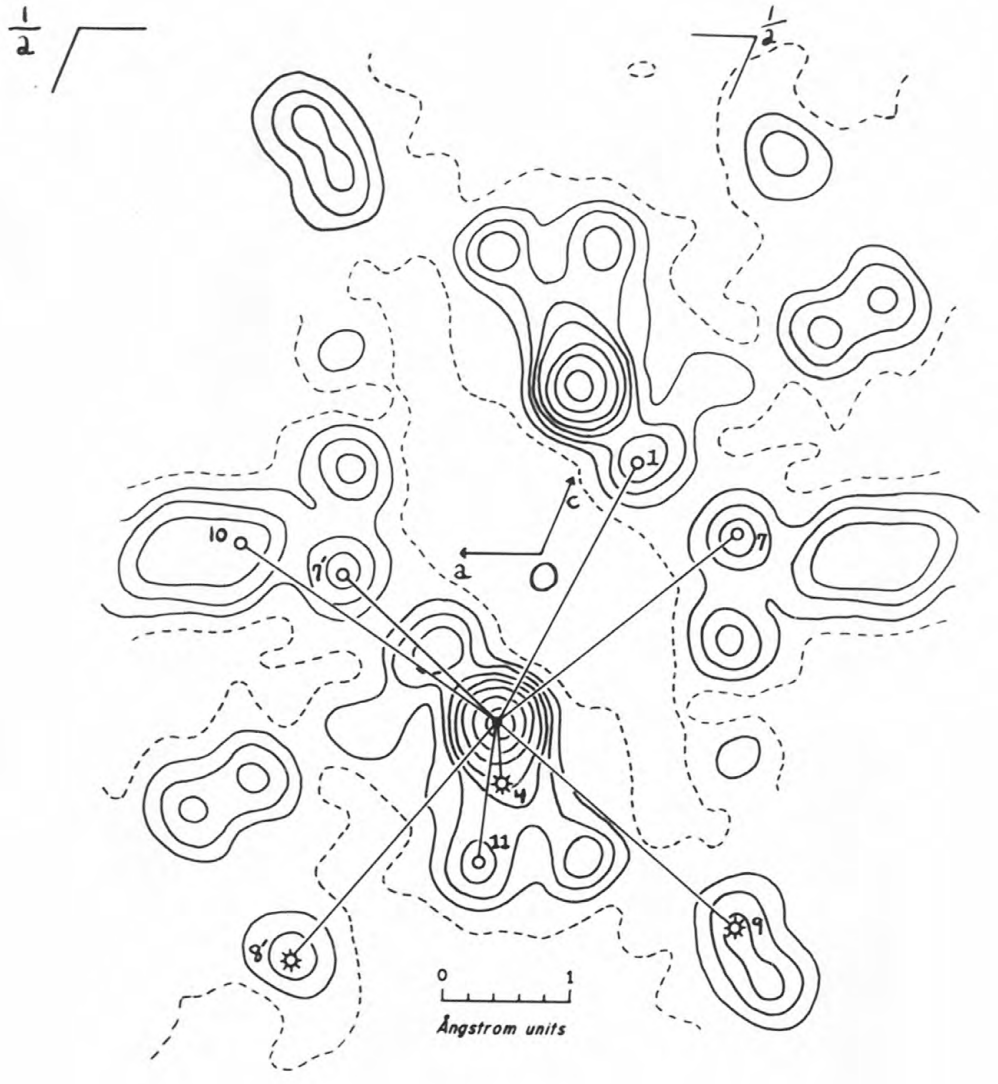

Figure 3

Figure 4

View of the structure along [001] showing a polyion-calcium-water column. Dashed lines indicate Ca-O bonds; dotted lines represent hydrogen bonds (Table 9). Polyions are shown with solid lines.

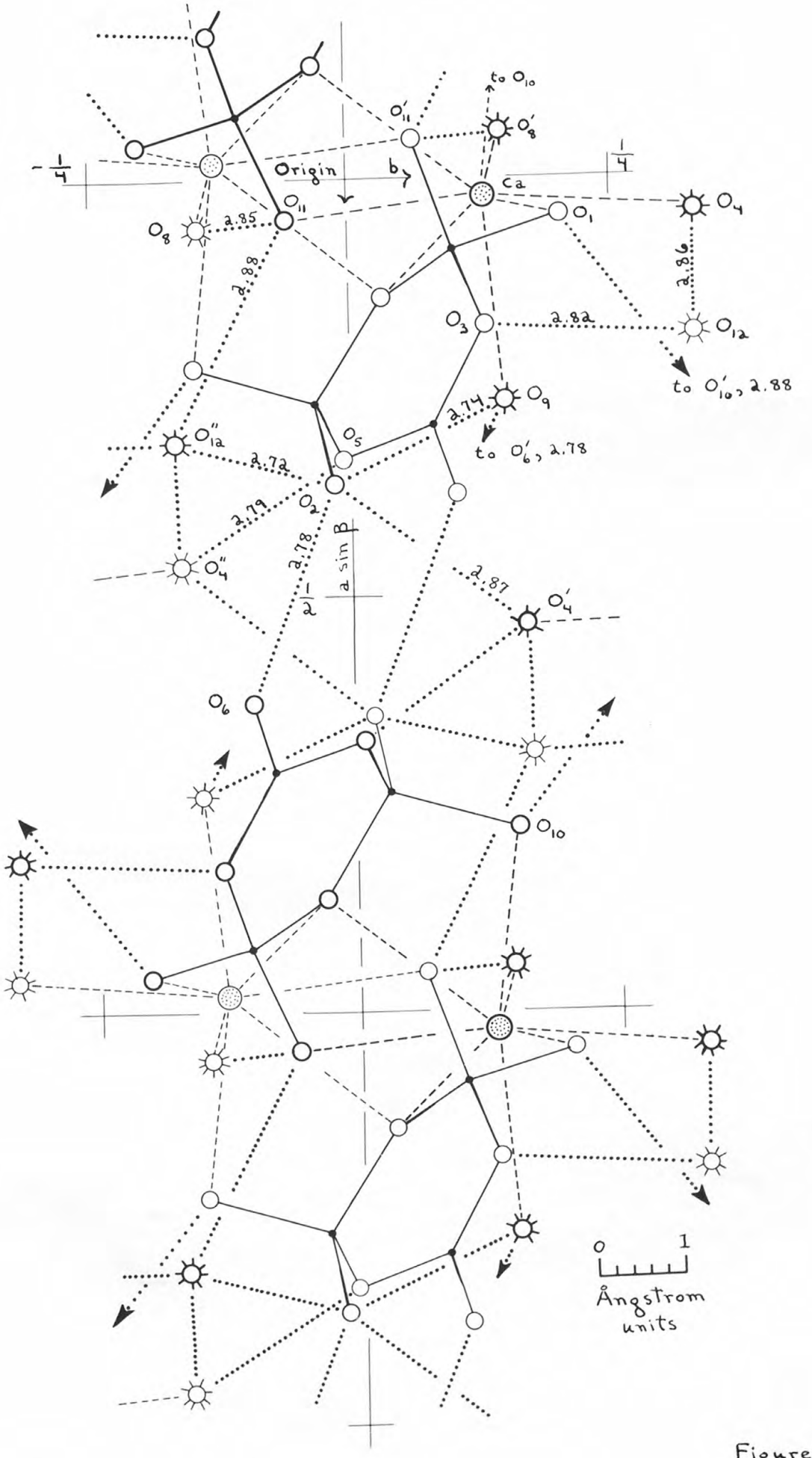
to O_{10}
O'_{11}
O'_8
Origin
b
Ca
O_{11}
O_8
2.85
2.88
O_1
O_4
2.86
O_3
2.82
O_{12}
to O'_{10}, 2.88
O_9
2.74
to O'_6, 2.78
O''_{12}
O_5
2.72
O_2
2.79
O''_4
2.78
a sin β
2.87
O'_4
O_6
O_{10}
0
1
Ångstrom units

Figure 4

Figure 5

View of the structure along [100] showing several columns and the inter-columnar bonds broken by the (001) and (010) cleavages. Dashed lines indicate Ca-O bonds; dotted lines represent hydrogen bonds (Table 9). Polyions are shown with solid lines.

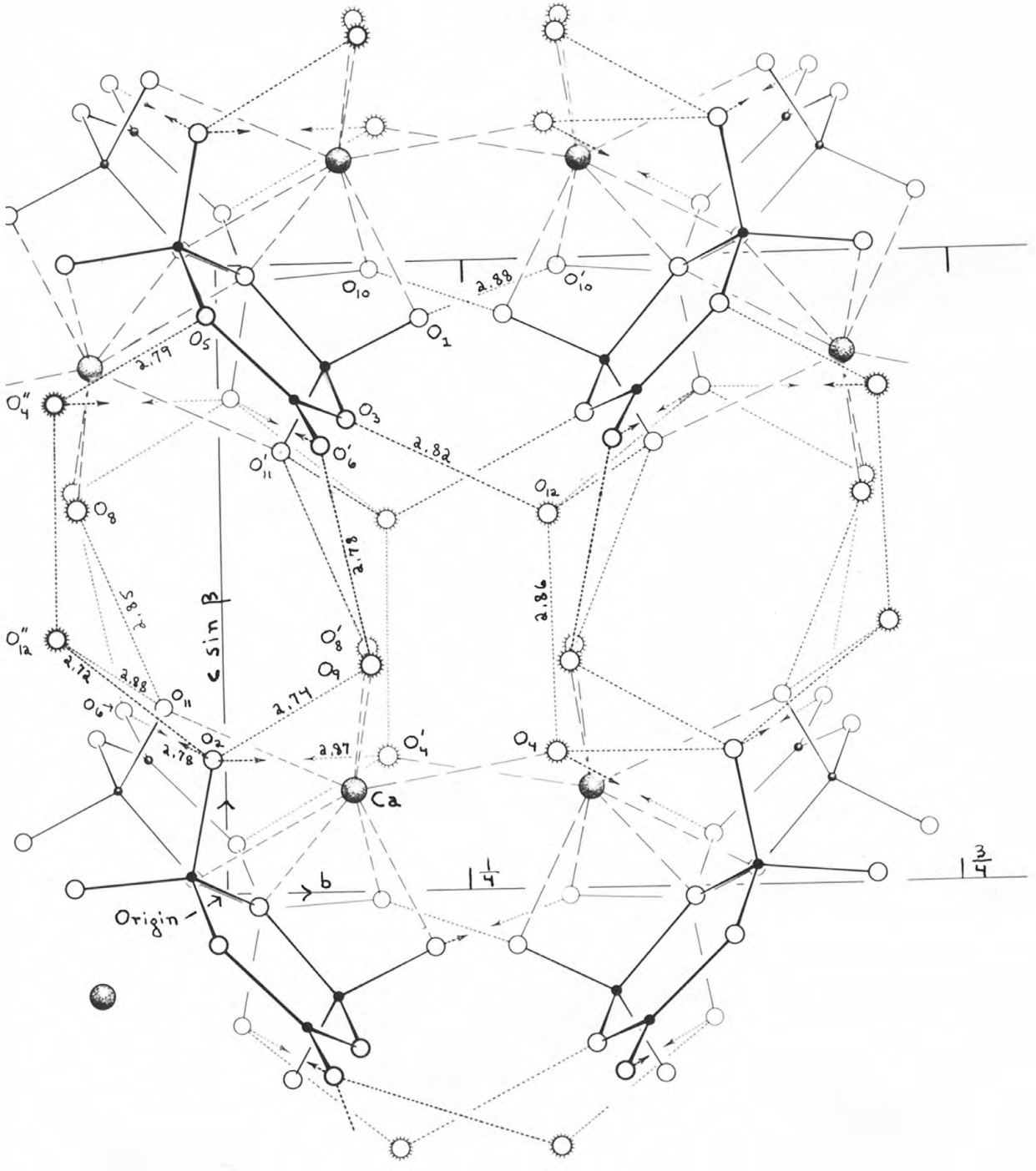
O10
O'10
2.88
O1
O5
2.79
O''4
O3
O'11
O'6
2.82
O12
O8
2.78
2.86
O''12
2.72
2.88
O11
c sin β
O'8
O9
2.74
O6
O2
2.78
2.97
O'4
O4
Ca
b
1/4
3/4
Origin

Figure 5.

References

Berghuis, J., Haanappel, IJ. M., Potters, M., Loopstra, B. O., MacGillavry, C. H. & Veenendaal, A. L. (1955). Acta Cryst. 8, 478.

Bokiĭ, G. B. (1937). Izvest. Akad. Nauk SSSR, Otdel. Mat. Estect. Nauk (Ser. Khim. No. 4), 871.

Booth, A. D. (1948). Fourier Technique in X-Ray Organic Structure Analysis (p. 62). Cambridge: University Press.

Buerger, M. J. (1951). Acta Cryst. 4, 531.

Christ, C. L. (1953). Amer. Min. 38, 411.

Christ, C. L. & Clark, J. R. (1956). Acta Cryst. 9, 830.

Christ, C. L., Clark, J. R. & Evans, H. T., Jr. (1958). Acta Cryst. ~~(in press).~~ 11, 761.

Clark, J. R. & Christ, C. L. (1957). Acta Cryst. 10, 776.

Cochran, W. (1948). J. Sci. Instrum. 25, 253.

Ibers, J. A. (1957). Acta Cryst. 10, 86.

Ingri, N., Lagerström, G., Frydman, M. & Sillén, L. G. (1957). Acta Chem. Scand. 11, 1034.

International Tables for X-Ray Crystallography, Vol. I (1952). Birmingham: The Kynoch Press.

Karle, J. & Hauptman, H. (1953). Acta Cryst. 6, 473.

Morimoto, N. (1956). Mineral. J. (Japan) 2, 1.

Palache, C., Berman, H. & Frondel, C. (1951). The System of Mineralogy, Vol. II, 7th ed. (p. 358). New York: John Wiley and Sons, Inc.

Poitevin, E. & Ellsworth, H. V. (1921). Can. Geol. Survey, Mus. Bull. No. 32, geol. ser. no. 39.

Schaller, W. T. (1916). U. S. Geol. Survey, Bull. 610, 35.

Viervoll, H. & Ögrim, O. (1949). Acta Cryst. 2, 277.

Wilson, A. J. C. (1942). Nature 150, 152.

Zachariasen, W. H. (1952). Acta Cryst. 5, 68.

Appendix I

The K(s) Calculation

The considerations involved in placing observed relative intensities, $F^2_{hk\ell}$, on an approximate absolute scale and in finding a preliminary temperature factor have been reviewed in Lipson and Cochran (1953). One method for treating the data in order to determine these factors was described by Karle and Hauptman (1953), and this method was used for the inyoite data.

First, the 5827 $F^2_{hk\ell}$ were listed according to increasing $s = (\sin\theta)/\lambda$ values and were divided into groups corresponding to intervals of s. Thirteen groups were formed, twelve of which contained about 465 terms each, while one group, for the interval $0<s<0.3$, contained only 222 terms. Within each group a K(s) value for the group was found from the relation

$$K(s) = \left(\sum_s \epsilon\, \sigma_2\right) \Big/ \left(\sum_s F_o^2(s)\right),$$

where $\sigma_2 = \sigma_2(s) = \sum_{j=1}^{N} f_j^2(s)$ and $\epsilon = \epsilon(s) = 2$ for all $hk\ell$ when $h = \ell = 0$ or when $k = 0$, while for all other $hk\ell$, $\epsilon = 1$. Table I gives the K(s) values which were found for each interval, and Fig. I shows the K(s) curve which was used during the preliminary stages of the determination.

Table I

Interval of s	K(s)
0 -0.3000	9.01
0.3001- .4415	13.68
.4416- .5213	15.25
.5214- .5828	23.07
.5829- .6335	28.93
.6336- .6781	27.21
.6782- .7176	32.00
.7177- .7518	41.18
.7519- .7835	45.42
.7836- .8133	53.20
.8134- .8423	62.49
.8424- .8710	61.49
.8711- .9000	86.28

Figure I

K(s) curve. Circles show the values listed in Table I.

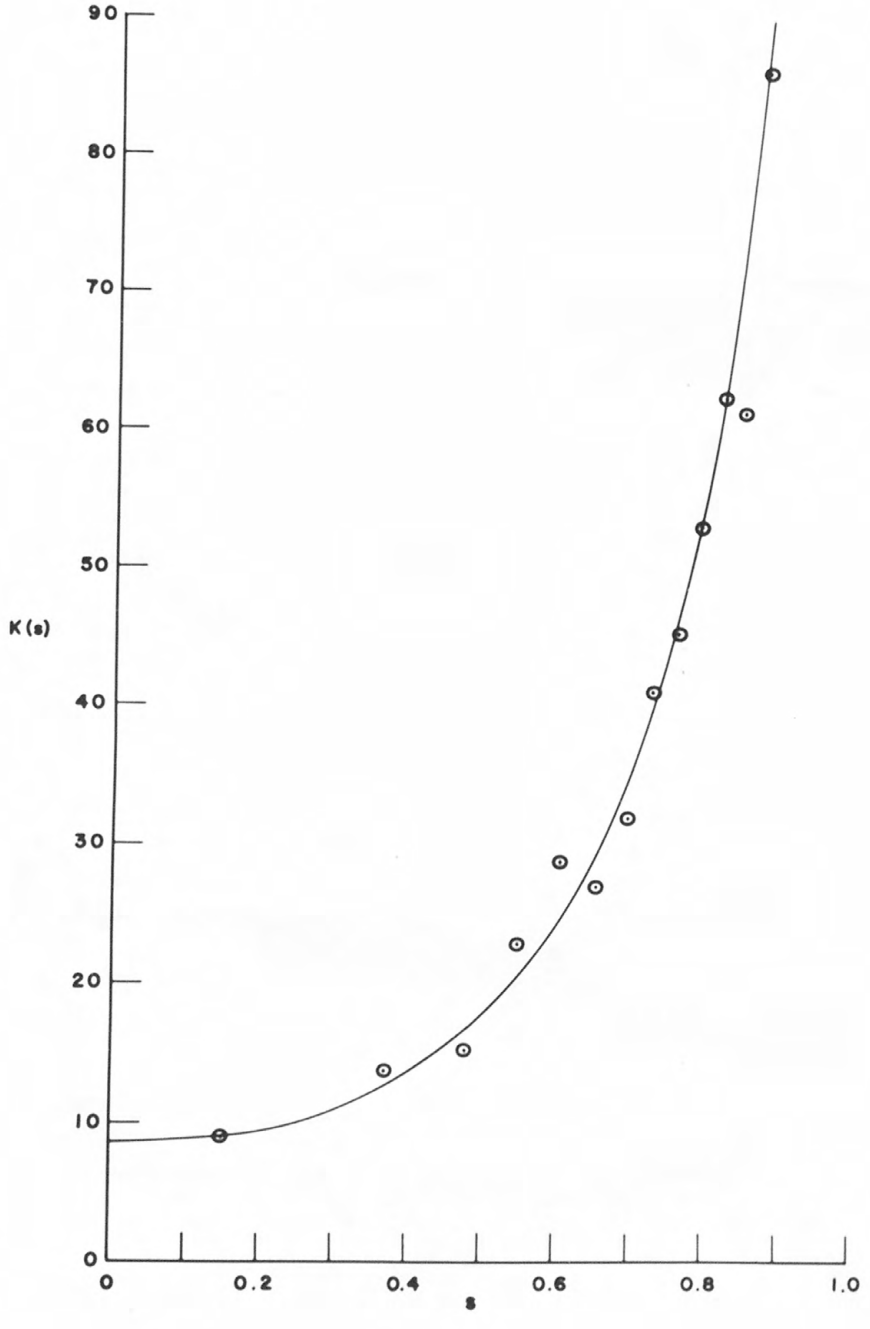

Figure I

Appendix II

Patterson Function

Introduction

Use of a new Fourier series, P(u,v,w), in crystal structure analysis was first described by Patterson (1935) and today the function is generally known as the Patterson function. It is usually written as follows:

$$P(u,v,w) = \frac{1}{V} \sum_{-\infty}^{\infty} \sum_{-\infty}^{\infty} \sum_{-\infty}^{\infty} |F(hkl)|^2 \cos 2\pi(hu+kv+lw),$$

where u,v,w in vector (Patterson) space are parallel to the x,y,z directions in crystal space, V is the cell volume, and $|F_{hkl}|^2$ are the observed intensities. The properties of the Patterson function and its many possible uses in crystal structure analysis have been discussed at length in the literature; excellent reviews on the subject are included in Lipson and Cochran (1953) and in James (1954).

Briefly, if a crystal contains an atom of atomic number Z_i, located at x_i, y_i, z_i in the crystal cell, and another atom of atomic number Z_j, located at x_j, y_j, z_j, the Patterson function for this crystal will have two peaks of weight Z_iZ_j, one with a maximum at $u = x_i-x_j$, $v = y_i-y_j$, $w = z_i-z_j$, and one with a maximum at $u = x_j-x_i$, $v = y_j-y_i$, $w = z_j-z_i$. There will also be a peak of

weight $Z_i + Z_j$ at u = 0, v = 0, w = 0. It follows that in the Patterson distribution a line drawn from the origin to a peak maximum is a vector which is equal to an interatomic vector in crystal space. Correct identification of at least some of these vectors is a prerequisite to use of the Patterson function in the solution of crystal-structure problem. The interpretation of the Patterson distribution for inyoite is outlined in this appendix.

Symmetry vectors in space group $\underline{P2_1/a}$

For a given space group it is possible to calculate those peak positions in the Patterson function which correspond to the interatomic vectors between crystallographically equivalent atoms. Table II lists for space group $\underline{P2_1/a}$ the following: peak weights, positions of peak maxima, and the symmetry element relating the two atoms which have the given interatomic vector.

Harker section

Examination of Table II shows that in Patterson space there occur on the plane $v = \frac{1}{2}$ peaks originating from interactions between crystallographically equivalent atoms related by the screw rotation. Harker (1936) first pointed out that this section at $v = \frac{1}{2}$ and similar sections in Patterson space contain useful information which can be related to the electron-density function. Any section of this type is now known as a Harker section and the

Table II

Peak Weight	Position of Peak Maximum			Symmetry Element
	u	v	w	
$2Z_j^a$	$\frac{1}{2}-2x$	$\frac{1}{2}$	$-2z$	2_1
	$\frac{1}{2}+2x$	$\frac{1}{2}$	$2z$	
$2Z_j^a$	$\frac{1}{2}$	$\frac{1}{2}-2y$	0	$\underline{a}$
	$\frac{1}{2}$	$\frac{1}{2}+2y$	0	
Z_j^a	$2x$	$2y$	$2z$	$\bar{1}$
	$-2x$	$-2y$	$-2z$	
	$2x$	$-2y$	$2z$	
	$-2x$	$2y$	$-2z$	

first four peaks listed in Table II are of the type often referred to as Harker peaks.

The expanded expression which was used for calculation of the inyoite Harker section is

$$P(u,\tfrac{1}{2},w) = \frac{1}{V}F^2(000) + \frac{2}{V}\left\{\sum_{h=1}^{\infty} p(0h0) + \sum_{h=1}^{\infty} C(h,0)\cos 2\pi hu + \sum_{l=1}^{\infty} C(0,l)\cos 2\pi lw + \sum_{h=1}^{\infty}\sum_{l=1}^{\infty}\left[C(h,l)+C(h,\bar{l})\right]\cos 2\pi hu \cos 2\pi lw - \sum_{h=1}^{\infty}\sum_{l=1}^{\infty}\left[C(h,l)-C(h,\bar{l})\right]\sin 2\pi hu \sin 2\pi lw\right\},$$

where u,v,w, and V have the same definitions as for the Patterson function, and $C(h,l) = p(h0l) + 2\sum_{k=1}^{\infty}(-1)^k p(hkl)$, the $p(hkl)$ being the "sharpened" intensities described in the text, i.e., $p(hkl) = [K(s)F^2(hkl)]/\hat{f}^2$.

There are sixteen atoms in the asymmetric unit of inyoite and each of these is expected to give rise to the first two Harker peaks listed in Table II. The Harker section for inyoite is shown in Fig. 1 of the text. The ratio of Ca-Ca to O-O Harker peaks is expected to be about 6:1. However, in the inyoite section, the ratio of the two largest peaks is 2:1. It is immediately evident that the section, in addition to the anticipated Harker peaks, must contain some or all of the following possibilities:

1) "non-Harker" peaks caused by Ca-O interatomic vectors which have a component along v that is approximately equal to $\frac{1}{2}$,

2) two or more O-O Harker peaks occurring at approximately the same location,

3) two or more "non-Harker" O-O peaks occurring at approximately the same location,

4) any combination of the various possibilities.

Correct identification of all the large peaks was thus virtually impossible without prior knowledge of the structure. This Harker section was therefore used principally to find the x- and z-coordinates of the calcium atom, the peaks marked A and B in Fig. 1 being checked against both location and size of peaks occurring on each of the three Patterson projections in order to identify A as the true Ca-Ca Harker peak. In later stages of the structure investigation the Harker section was also used to some extent for checking postulated oxygen positions by looking for the appearance of the corresponding O-O Harker peaks.*

Patterson projections

The expanded expressions which were used to calculate the three inyoite Patterson projections, each taken on a plane normal to a crystallographic axis, are given below. As before u, v, w and V have the same definitions given for the Patterson function, and p(hkℓ) are the "sharpened" intensities described in the text.

*The section was not as helpful in this respect as it might have been because a machine error during calculation had resulted in omission from the computation of all C(h,ℓ) with positive ℓ and h,$\ell \neq 0$. The omission was not discovered until after the structure had been determined; fortunately it did not affect the essential features of the section.

(1) For the projection on a plane normal to the c axis,

we have

$$P_w(u,v) = \frac{c}{V} F^2(000) + \frac{2c}{V} \left\{ \sum_{h=1}^{\infty} p(h00) \cos 2\pi hu + \sum_{k=1}^{\infty} p(0k0) \cos 2\pi kv \right\} + \frac{4c}{V} \left\{ \sum_{h=1}^{\infty} \sum_{k=1}^{\infty} p(hk0) \cos 2\pi hu \cos 2\pi kv \right\} .$$

(2) For the projection on a plane normal to the b axis,

we have

$$P_v(u,w) = \frac{b}{V} F^2(000) + \frac{2b}{V} \left\{ \sum_{h=1}^{\infty} p(h00) \cos 2\pi hu + \sum_{l=1}^{\infty} p(00l) \cos 2\pi lw + \sum_{h=1}^{\infty} \sum_{l=1}^{\infty} [p(h0l) + p(h0\bar{l})] \cos 2\pi hu \cos 2\pi lw - \sum_{h=1}^{\infty} \sum_{l=1}^{\infty} [p(h0l) - p(h0\bar{l})] \sin 2\pi hu \sin 2\pi lw \right\} .$$

(3) For the projection on a plane normal to the a axis, we have

$$P_u(v,w) = \frac{a}{V} F^2(000) + \frac{2a}{V} \left\{ \sum_{k=1}^{\infty} P(0k0) \cos 2\pi k v + \sum_{l=1}^{\infty} P(00l) \cos 2\pi l w \right\} + \frac{4a}{V} \left\{ \sum_{k=1}^{\infty} \sum_{l=1}^{\infty} P(0kl) \cos 2\pi k v \cos 2\pi l w \right\}.$$

The three Patterson projections for inyoite are shown in Figs. IIa, IIb, and IIc of this appendix; Ca-Ca peaks have been labeled on each projection. Coordinates for the calcium atom were calculated from these peak maxima according to the relations shown in Table II. The values obtained from each projection and from the Harker section have been summarized in Table 1 of the text; the agreement was excellent, and an average set of x-, y-, z-coordinates was chosen for the first structure factor calculations.

Minimum-function maps

Numerous methods have been suggested for recovering the electron-density function from the corresponding Patterson function. A critical survey of these methods is given in Lipson and Cochran (1953). One such technique which has been used in recent years with increasing frequency for crystal-structure determination is the superposition method. This technique is based on the possibility of identifying one or more single Patterson peaks, such as

Figure IIa

Sharpened $P_w(u,v)$. Contours at arbitrary levels, intervals of 100 between the first three contours and 200 thereafter. A is the Ca-Ca inversion peak; B is the Harker Ca-Ca screw rotation peak; C is the Harker Ca-Ca glide reflection peak.

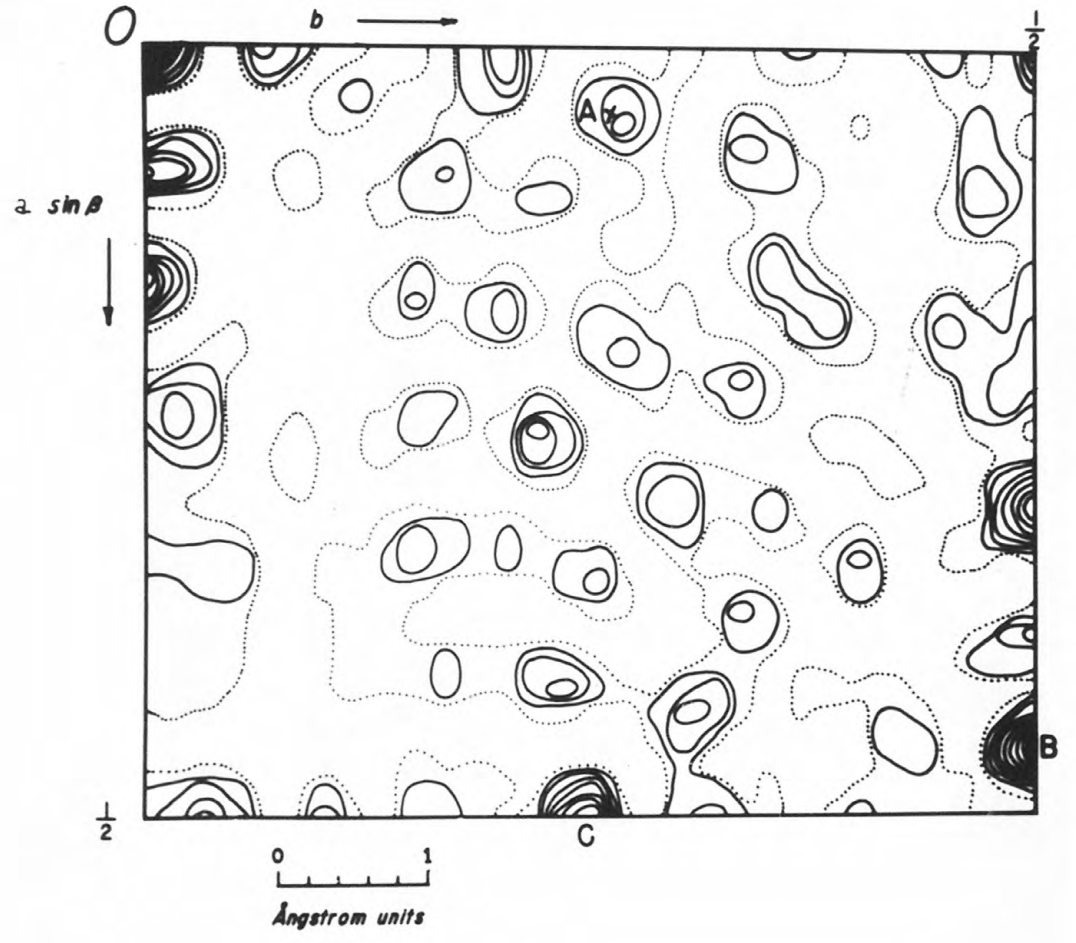

Figure IIa

Figure IIb

Sharpened $P_v(u,w)$. Contours at arbitrary levels, intervals of 50. A is the Ca-Ca inversion peak.

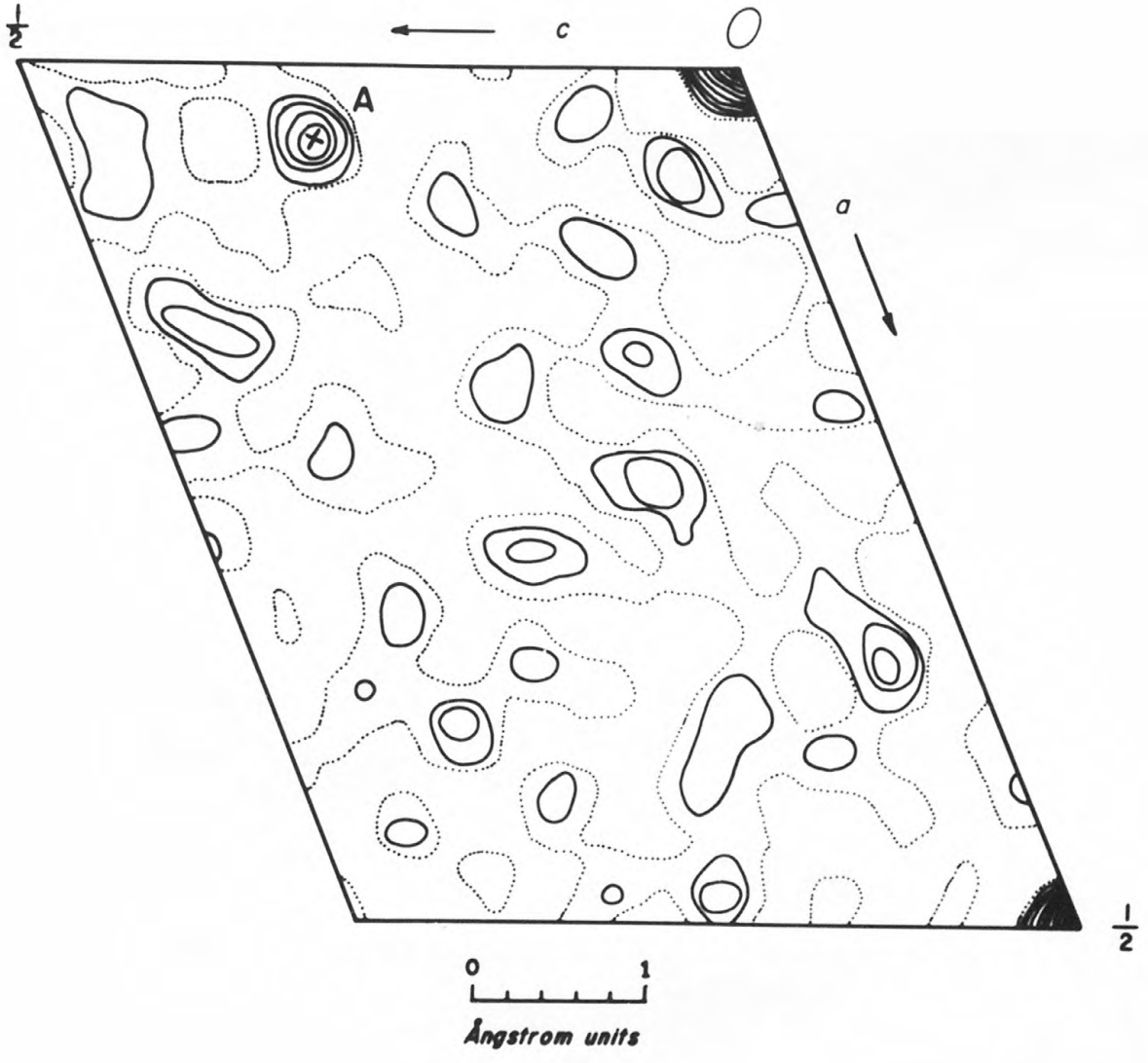

Figure IIb

Figure IIc

Sharpened $P_u(v,w)$. Contours at arbitrary levels, intervals of 100 between the first three contours and 200 thereafter (except around peaks A, B, C where intervals are all 200). A is the Ca-Ca inversion peak; B is the Harker Ca-Ca screw rotation peak; C is the Harker Ca-Ca glide reflection peak.

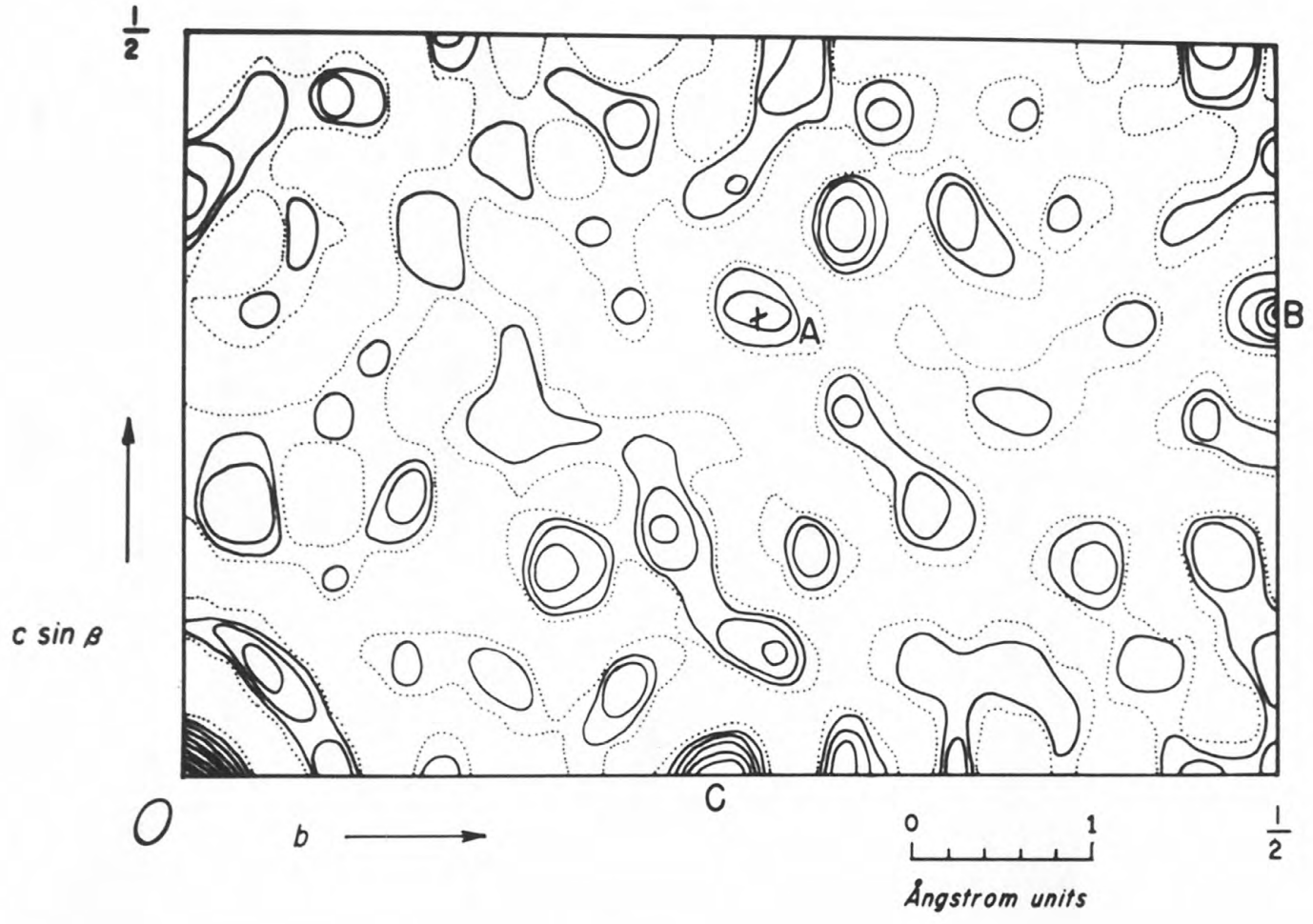

Figure IIc

the last four listed in Table II. Any single peak may then be used as a basis for superposition of two identical Patterson maps, the origin peak of one map being placed on a selected single Patterson peak in the other map and an appropriate combination function being applied to obtain an approximate electron-density map. Theoretically the combination function should produce regions of density corresponding to atomic positions because the superposition, as described, seeks out all interatomic vectors between the selected atom and other atoms in the structure, while the combination function maps the regions of density near end-points of these vectors.

In applying this technique to inyoite, the procedure described by Buerger (1951) was used; the combination function recommended by him is the minimum function, which, as its name implies, always selects the lower point of the two superposed distributions for production of the approximate electron-density map (M map). Each Patterson projection was traced twice; for each contour level a different color was used so that the levels could be readily identified and the minimum rapidly found following the superposition. Identification of all Ca-Ca peaks in the Patterson projections had been made as previously described (see Figs. IIa, IIb, IIc), and the inversion Ca-Ca peak at u = 2x, v = 2y, w = 2z was selected as a basis for the superposition. The origin of the given M map was taken at a center of symmetry, located at the midway point of the vector in the Patterson projection between the origin and the

Ca-Ca peak. Because of the glide reflection, a second superposition could be performed for the projections on planes normal to the a and c axes. Following Buerger's notation, the M map obtained from the single superposition possible for the projection on a plane normal to the b axis has been called $M_{2y}(x,z)$, while the others, based on two superpositions, have been called, respectively, $M_{4z}(x,y)$ and $M_{4x}(y,z)$.

The three M maps are shown in Figs. IId, IIe, IIf and should be compared with two electron-density projections, illustrated in Figs. IIg and IIh, which were described in the text as the ones calculated using terms which could be considered fixed in sign on the basis of the calcium contribution to the structure factors. Because these projections (No. 1) and the M maps all depend on the calcium position, they should be, and are, similar in detail. A deceiving clarity of detail occurs in the M maps as a result of the "sharpened" coefficients used in the Patterson analyses. The value of the sharpening is open to question since, while it does provide good resolution, it may shift peak maxima and introduce some false peaks, as, e.g., in the locations of diffraction maxima around the atoms. A direct comparison of the effects produced by using "sharpened" coefficients is given in Fig. IIh (unsharpened ρ_y No. 1) and Fig. IIi ("sharpened" ρ_y No. 1).

Sketches of the $[B_3O_3(OH)_5]^{-2}$ polyion on both the M maps and the ρ No. 1 show the final orientation of the atoms and permit convenient comparison of all these maps with the final electron-

Figure IId

$M_{4z}(x,y)$. Correct orientation of polyion is shown. Final atomic sites are marked: open circles for oxygens or hydroxyl oxygens; spoked circles for water oxygens. Compare to Figs. 2 (text) and IIg.

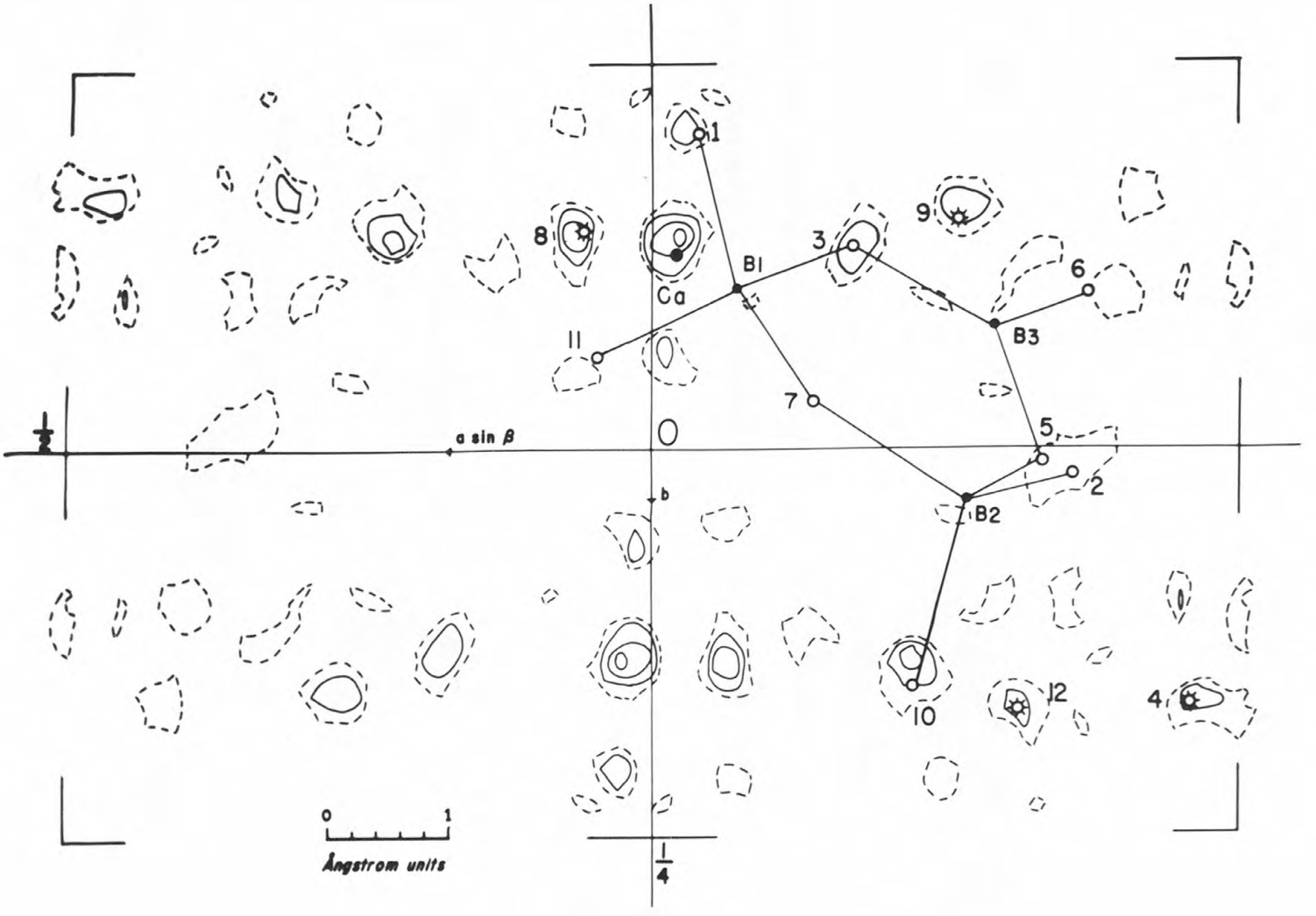

Figure IId

Figure IIe

$M_{ay}(x,z)$. Correct orientation of polyion is shown. Final atomic sites are marked: open circles for oxygens or hydroxyl oxygens; spoked circles for water oxygens. Compare to Figs. IIIa and IIi.

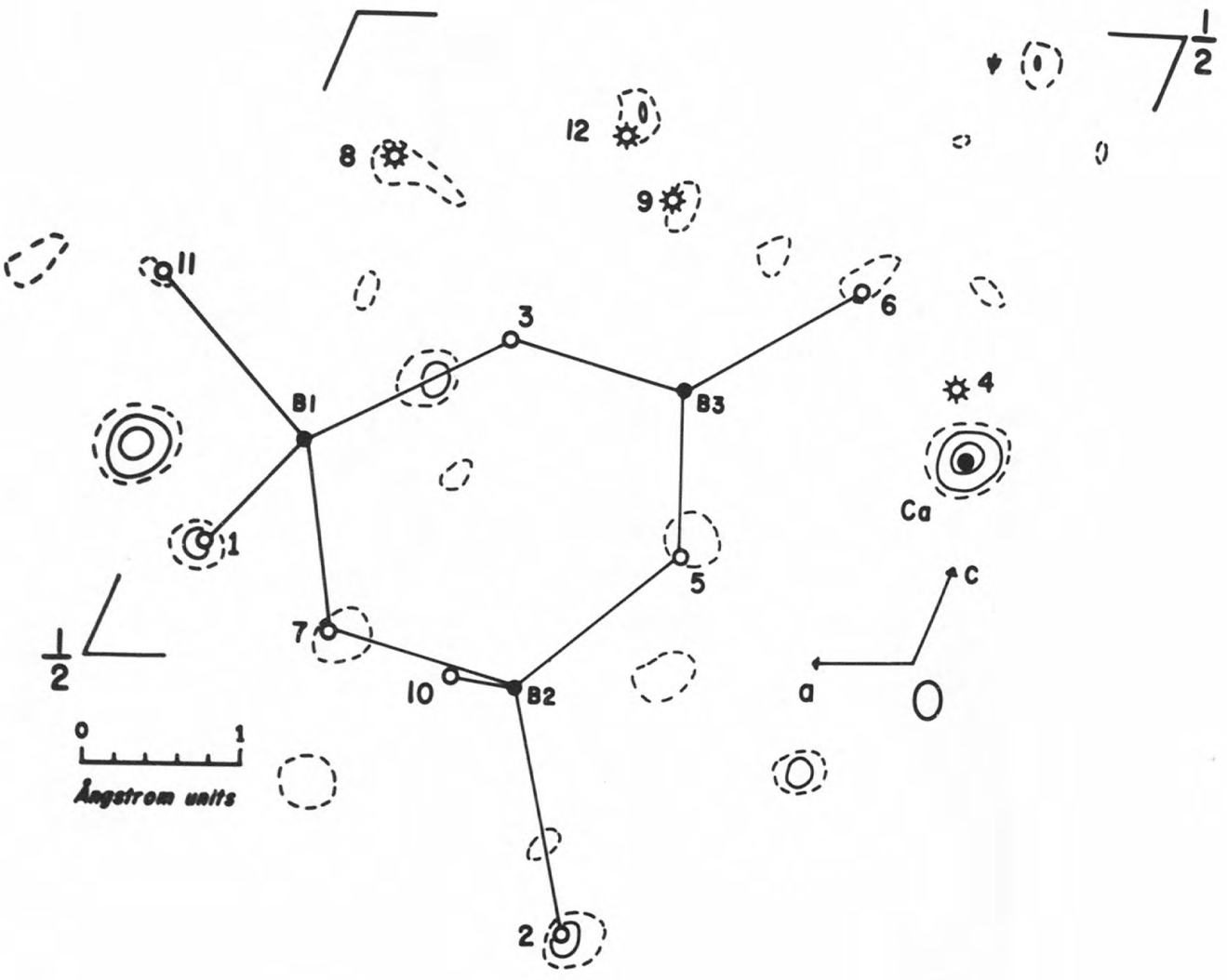

Figure IIe

Figure IIf

$M_{4x}(y,z)$. Correct orientation of polyion is shown. Final atomic sites are marked: open circles for oxygens or hydroxyl oxygens; spoked circles for water oxygens. Compare to Fig. IIIb.

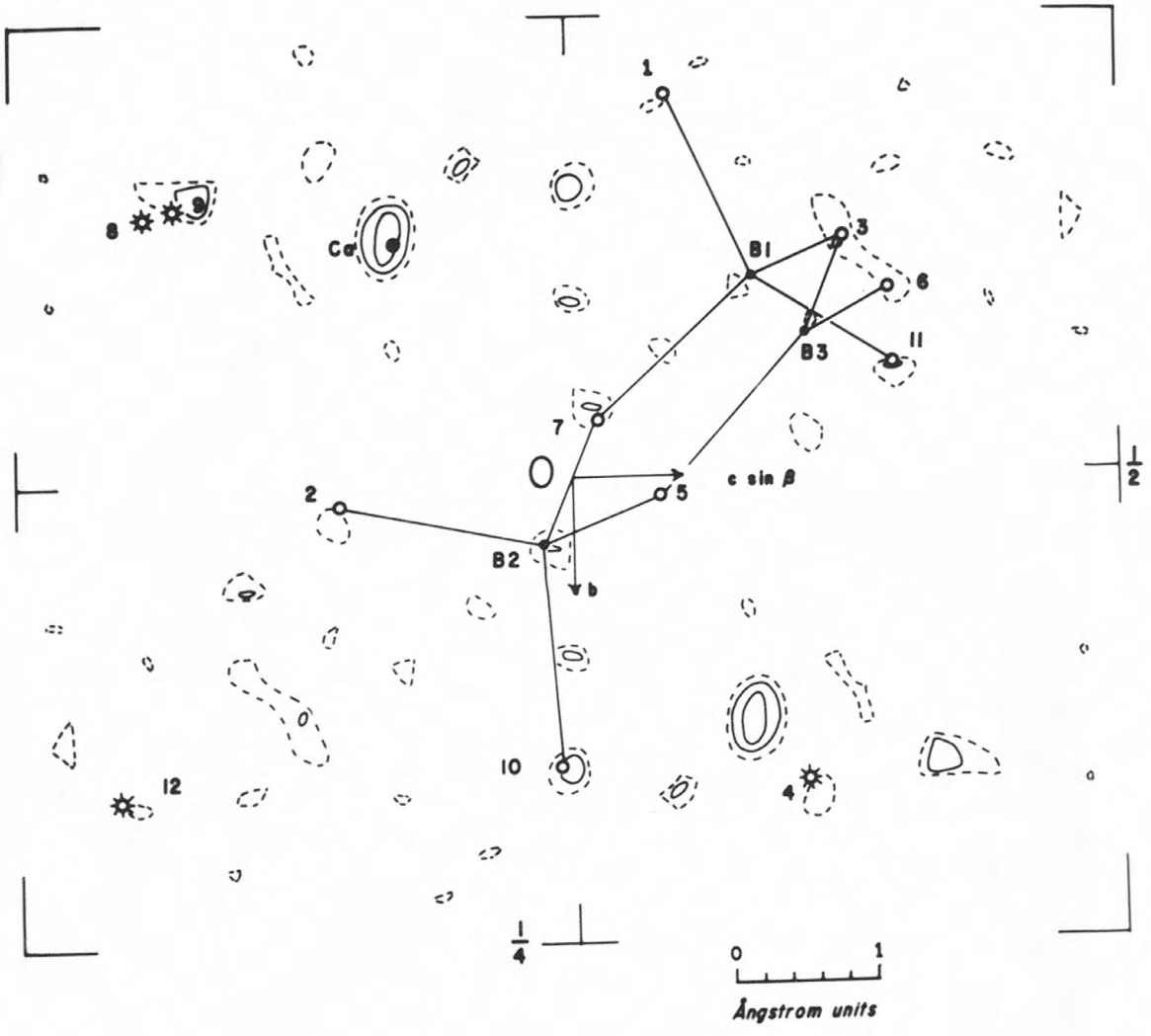

Figure IIf

Figure IIg

$\rho_z(x,y)$ No. 1, calculated using F_o coefficients with signs determined from Ca contribution to S.F. Contours at arbitrary levels, intervals of 10 except around Ca where intervals are 50. Correct orientation of polyion is shown. Final atomic sites are marked: open circles for oxygens or hydroxyl oxygens; spoked circles for water oxygens. Compare to Figs. 2 (text) and IId.

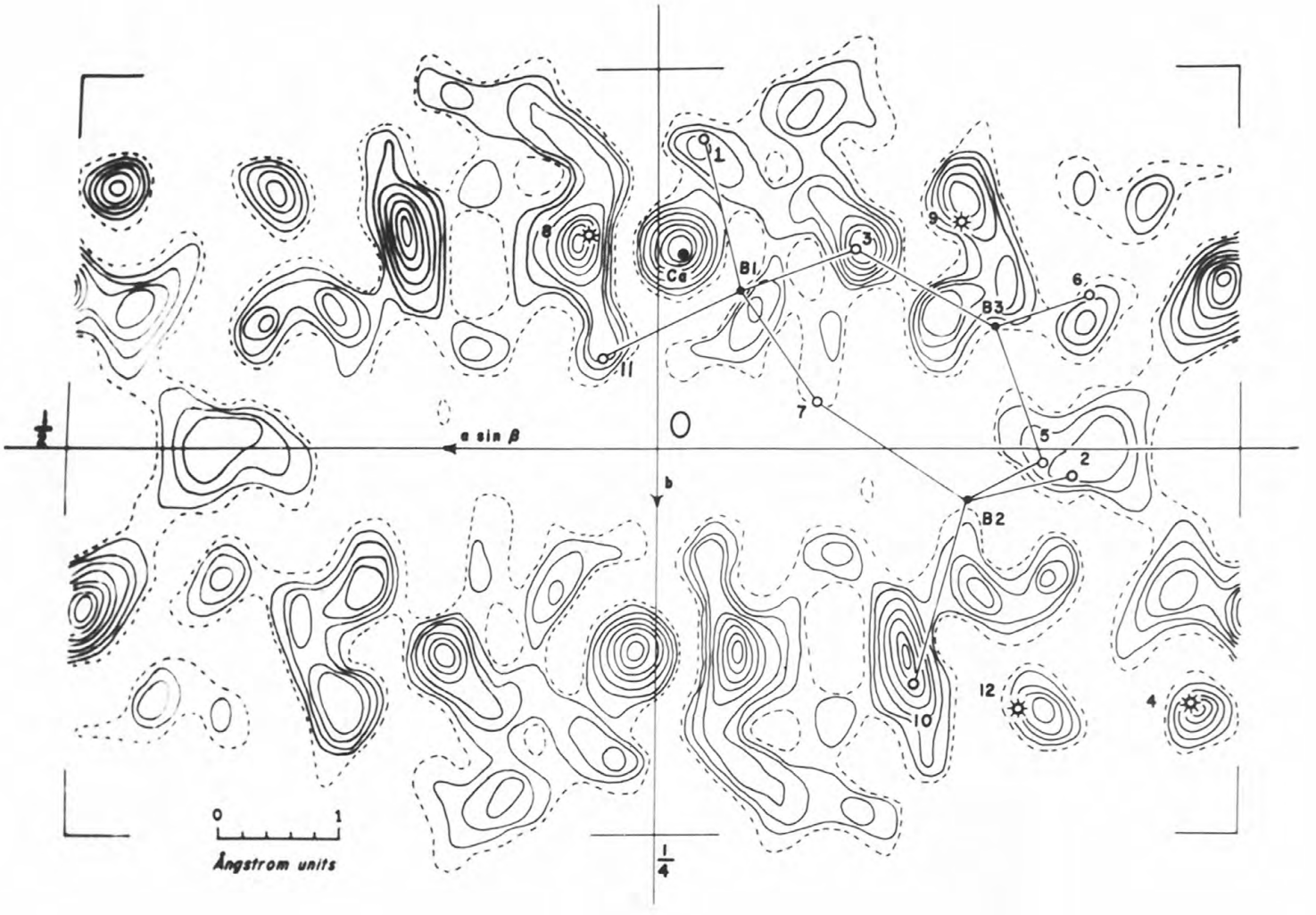

Figure II 8

Figure IIh

$\rho_y(x,z)$ No. 1, calculated using F_o coefficients with signs determined from Ca contribution to S.F. Contours at arbitrary levels, intervals of 20, except around Ca after the third contour, intervals of 100. Correct orientation of polyion is shown. Final atomic sites are marked: open circles for oxygens or hydroxyl oxygens; spoked circles for water oxygens. The peak labeled ψ is spurious. Compare to Figs. IIIa, IIe, and IIi.

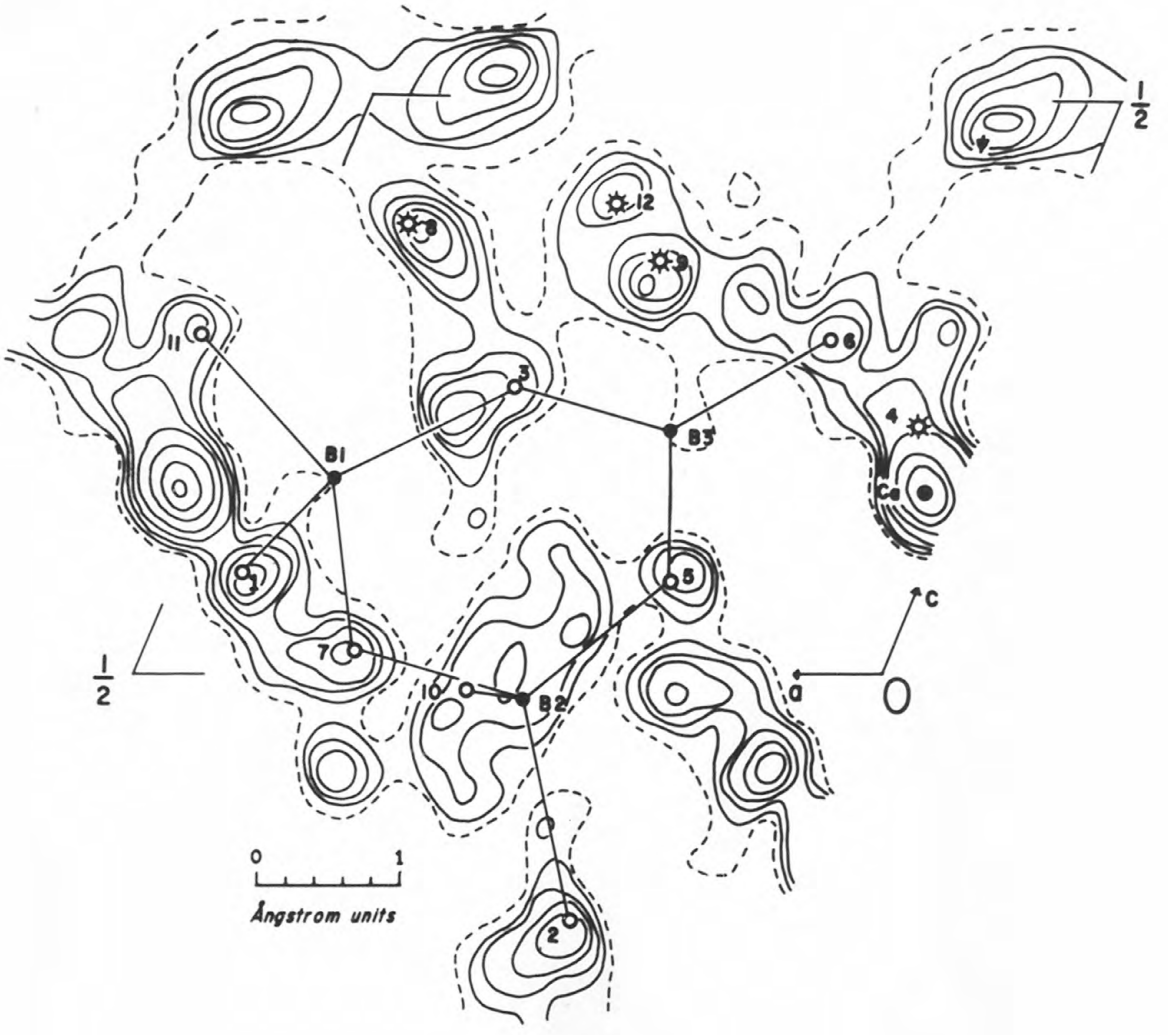

Figure IIh

Figure IIi

$\rho_y(x,z)$ No. 1, calculated using E_o coefficients with signs determined from Ca contribution to S.F. Contours at arbitrary levels, intervals of 100 except around Ca where intervals are 200 for the first four contours and 500 thereafter. Correct orientation of the polyion is shown. Final atomic sites are marked: open circles for oxygens or hydroxyl oxygens; spoked circles for water molecules. The peak labeled ψ is spurious. Compare to Figs. IIIa, IIe, and IIh.

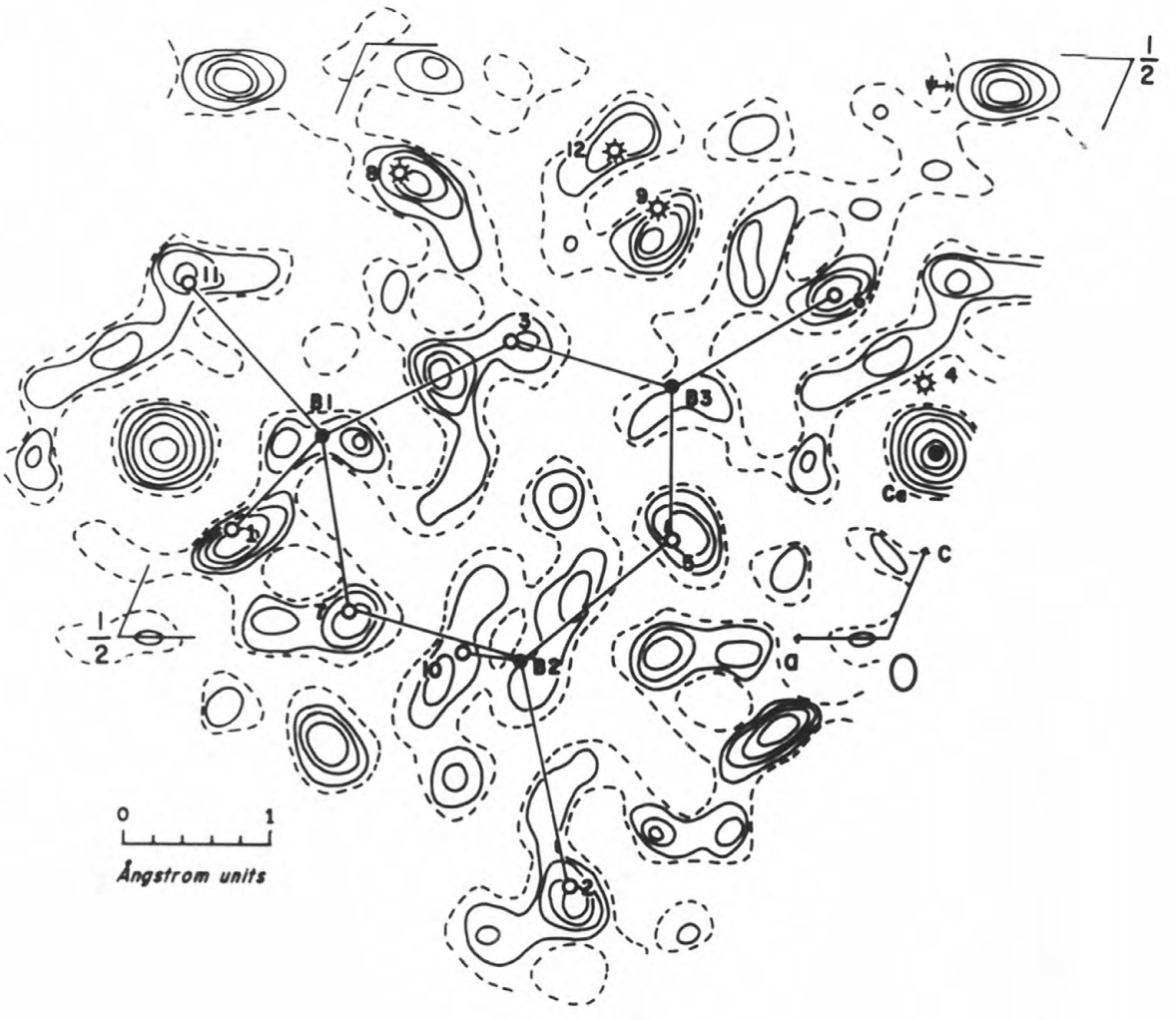

Figure II c

density projections shown in Figs. 2 and 3 of the text and in Figs. IIIa, IIIb, Appendix III. Several sources of difficulty in the interpretation of the first maps are apparent. One problem was the presence of false peaks, an example being the peak labeled ψ on M_{ay} (Fig. IIe) and on ρ_y No. 1 (Figs. IIh, IIi). This peak was the false one, referred to in the text, which was eliminated only after examination of individual h0ℓ structure-factor contributions. Its position was an especially difficult one to eliminate because the x-coordinate of that peak on ρ_y agreed with the x-coordinate of a peak on ρ_z, placing the "oxygen" at a reasonable (2.4 A) coordination distance to the calcium. A second problem was the absence of peaks where atoms actually existed. Such absences were not surprising in the case of the boron atoms, but the open space on M_{4z} (Fig. IId) and on ρ_z No. 1 (Fig. IIg) where O_7 belonged was a considerable obstacle. Finally, the numerous shifts of the M map peak maxima from the correct atomic locations resulted in poor agreement between observed and calculated structure factors even when the positions were approximately right. For a structure containing this number of atoms there is no doubt that immediate application of phase-determination procedures (Appendix V) would have been a more efficient method for solving the structure.

Appendix III

Calculations in Space Group P2 /a

Structure factors

The structure factors, $F_{hk\ell}$, were calculated from the expressions given below, where f_j is the atomic scattering factor of the jth atom which is located in the cell at x_j, y_j, z_j. In each case N is the total number of atoms in the cell; for inyoite, N = 64, not counting the hydrogen atoms.

1) For hkℓ reflections with h+k = 2n,

$$F_{hk\ell} = 4 \sum_{j=1}^{N/4} f_j \cos 2\pi(hx_j+\ell z_j)\cos 2\pi k y_j.$$

2) For hkℓ reflections with h+k = 2n+1,

$$F_{hk\ell} = -4 \sum_{j=1}^{N/4} f_j \sin 2\pi(hx_j+\ell z_j)\sin 2\pi k y_j.$$

In Table 3 of the text, calculated $F_{hk\ell}$ are compared to observed $F_{hk\ell}$ for all zone reflections. In order to check agreement of some general $F_{hk\ell}$ terms, the data contained within the reciprocal sphere for Cu$K\alpha$ radiation (radius s = 0.65$\mathring{A}^{-1}$) were arranged in order of increasing s and $F_{hk\ell}$ calculated for every tenth term from the atomic coordinates of Table 2, column 4. The three zone values for B and k given in Table 2, column 4, were averaged and the average values used to obtain the F_c and F_o listed in Table III, which omits

Table III

Comparison of observed and calculated structure factors for selected general hkℓ terms. Calculated $F_{hk\ell}$ are based on the atomic coordinates of Table 2, Column 4 (text). Average isotropic temperature factor B = 1.00Å^2 ; scaling factor k = 3.1. Residual for this group, 0.17.

hkℓ	Fo	Fc
1 5 1	51	40-
1 8 1	10	9
1 11 1	11	8-
3 4 1	26	24
3 8 1-	10	10-
3 12 1	16	25
3 12 1-		3-
3 13 1-	8	9-
4 10 1	15	19
4 10 1-	27	24-
4 13 1-	8	9
5 4 1	5	3
6 10 1-	13	13-
7 8 1	5	6-
8 3 1	17	20-
8 9 1-	6	9-
9 1 1	17	11-
9 3 1-	18	15-
9 4 1-	6	10
9 6 1	5	5
9 9 1-	8	15
10 5 1-	12	18
11 4 1-	8	9-
11 8 1-		1
12 1 1-		1
1 3 2-	26	22
1 9 2	17	16-
1 13 2	14	16
2 1 2	22	18-
2 5 2	15	17-
2 14 2		2-
3 6 2-	58	67-
3 12 2-	7	10
4 9 2	23	16-
4 9 2-	13	18
4 14 2-	3	0
5 2 2	32	36-
5 9 2	18	18-
5 10 2		0
5 14 2-	11	10-
6 3 2	8	9-
8 12 2-	14	16-
12 4 2-		8-
1 3 3-	26	24-
1 4 3-	25	20-
1 5 3	82	76
1 13 3	18	19
2 1 3-	56	32
2 2 3	11	12-
2 9 3		2-
3 8 3	18	15-
3 8 3-		7
4 6 3	22	25
4 13 3		3
5 3 3-	51	48
5 8 3-	16	19
5 9 3-	10	8-
6 8 3-	4	1-
7 3 3-	13	19
7 4 3-		1-
8 2 3-	28	26
9 1 3-	28	30-
9 5 3	12	13
9 6 3-		1-
9 10 3-	17	25
9 11 3-		6
11 2 3-	35	30
12 2 3-		4-
1 2 4	39	38
1 3 4	62	56
1 3 4-	41	34
1 10 4	21	24
1 14 4	14	13-
2 2 4	24	24-
2 4 4	23	21
2 4 4-	42	39
3 10 4-	17	22-
4 5 4-	26	30
4 12 4	11	14
5 1 4	23	28-
5 6 4-	18	21
6 1 4-	8	4
6 7 4-	24	26
6 9 4	12	10
7 2 4	8	4
8 2 4	9	11-
8 3 4	15	13
8 7 4	12	16-
9 3 4	13	15-
9 5 4-	27	25
9 7 4-	12	4-
11 5 4-	22	25
11 7 4-	10	8-
11 9 4-		2-
1 6 5-	19	17
1 11 5	9	15-
1 11 5-		0
1 12 5-	13	15
2 2 5	5	3-
2 5 5	16	14-

hkℓ	F_o	F_c
2 6 5	10	12
2 7 5	20	23-
2 8 5-	13	21
3 5 5-	10	15-
3 13 5-	10	12
4 2 5-	18	13-
4 7 5		1-
4 8 5	10	14
5 3 5	16	16-
5 9 5-	6	10
6 3 5-	17	17-
6 12 5-	13	16
8 7 5-	3	2-
8 10 5-	6	6
9 3 5-	11	12
9 4 5-		1
9 9 5-	11	13-
1 2 6		2
1 2 6-	18	13-
1 4 6-	6	9
1 6 6	21	17-
1 11 6-	10	7-
2 6 6-	8	7-
3 3 6-	14	9-
3 9 6	6	8-
4 10 6-	3	4-
5 2 6-	29	28-
6 1 6	12	12
7 8 6-	6	12-
7 12 6-		0
8 2 6-	21	24-
9 7 6-		2
10 2 6-	23	20-
11 1 6-	10	3-
11 3 6-		4-
11 5 6-	7	9
12 6 6-		1
1 2 7		0
2 5 7	6	7
2 7 7-		2-
3 7 7-	4	6
4 6 7		6
4 10 7-	6	7-
5 2 7	15	13-
7 5 7-	7	9
7 11 7-	16	21-
8 4 7-	32	29-
8 8 7-	15	20
9 2 7-	26	19-
9 3 7-	31	42-
10 5 7-		1-
11 5 7-	17	18-
1 1 8		0
1 6 8	17	20
1 6 8-	23	26-
1 7 8	10	12
1 8 8	7	10-
2 1 8	23	20-
3 1 8	13	12-
4 3 8	8	8-
4 6 8-		3
6 1 8-	33	32
9 2 8-		6
9 4 8-		9
11 6 8-		1
1 3 9	13	18
2 3 9-	9	7
2 7 9-	17	24-
4 1 9-	8	5
4 6 9-	8	6-
5 7 9-		9
6 1 9-	11	10
6 3 9-	18	17
8 2 9-		1-
8 7 9-	23	31-
9 2 9-	12	14
9 6 9-	24	23-
2 3 10-	10	13
3 4 10-	11	14
4 4 10-	16	20
4 6 10-		4
4 9 10	9	15
5 4 10-		7
6 4 10-	20	20
8 4 10-		15

reflections already included in Table 3. The residual for the group of Table III is 0.17.

Residual

The residual, R, is obtained from the formula, $R = \sum \left| |F_o| - |F_c| \right| \Big/ \sum |F_o|$. In calculating the values of R for inyoite, the summation included all $F_{hk\ell}$ where $|F_o| > 0$.

Electron-density projections

Each electron-density projection was taken on a plane normal to a crystallographic axis. The expanded expression used for each calculation is given below. In all the relations the following definitions hold: a, b, c are the cell edges, V is the cell volume, $F_{hk\ell}$ are the observed absolute structure factors. Each projected cell edge was divided into sixty parts and the Fourier series was evaluated at each of these points for the asymmetric portion of the projection.

1) Projection on a plane normal to c:

$$\rho_z(x,y) = \frac{c}{V} F(000) + \frac{2c}{V} \left\{ \sum_{h=1}^{\infty} F(h00) \cos 2\pi hx + \sum_{k=1}^{\infty} F(0k0) \cos 2\pi ky \right\}$$

$$+ \frac{4c}{V} \left\{ \sum_{\substack{h=1 \\ h+k=2n}}^{\infty} \sum_{k=1}^{\infty} F(hk0) \cos 2\pi hx \cos 2\pi ky \right.$$

$$\left. - \sum_{\substack{h=1 \\ h+k=2n+1}}^{\infty} \sum_{k=1}^{\infty} F(hk0) \sin 2\pi hx \sin 2\pi ky \right\}.$$

2) Projection on a plane normal to b:

$$\rho_y(x,z) = \frac{b}{V} F(000) + \frac{2b}{V} \left\{ \sum_{h=1}^{\infty} F(h00) \cos 2\pi hx + \sum_{l=1}^{\infty} F(00l) \cos 2\pi lz \right\}$$

$$+ \frac{2b}{V} \left\{ \sum_{h=1}^{\infty} \sum_{l=1}^{\infty} \left[F(h0l) + F(h0\bar{l}) \right] \cos 2\pi hx \cos 2\pi lz \right.$$

$$\left. - \sum_{h=1}^{\infty} \sum_{l=1}^{\infty} \left[F(h0l) - F(h0\bar{l}) \right] \sin 2\pi hx \sin 2\pi lz \right\}.$$

3) Projection on a plane normal to a:

$$\rho_x(y,z) = \frac{a}{V} F(000) + \frac{2a}{V} \left\{ \sum_{k=1}^{\infty} F(0k0) \cos 2\pi ky + \sum_{l=1}^{\infty} F(00l) \cos 2\pi lz \right\}$$

$$+ \frac{4a}{V} \left\{ \sum_{\substack{k=1 \\ k=2n}}^{\infty} \sum_{l=1}^{\infty} F(0kl) \cos 2\pi ky \cos 2\pi lz \right.$$

$$\left. - \sum_{\substack{k=1 \\ k=2n+1}}^{\infty} \sum_{l=1}^{\infty} F(0kl) \sin 2\pi ky \sin 2\pi lz \right\}.$$

Figs. 2 and 3 of the text illustrate two final electron-density projections, $\rho_z(x,y)$ and $\rho_y(x,z)$, the first showing the orientation of the $[B_3O_3(OH)_5]^{-2}$ polyion and the other showing Ca-O coordination. Fig. IIIa repeats $\rho_y(x,z)$ with the polyion orientation illustrated, and Fig. IIIb shows the polyion as it appears on the final $\rho_x(y,z)$.

Figure IIIa

Final $\rho_y(x,z)$. Contours at intervals of $4e/Å^2$ except around Ca where intervals become $10e/Å^2$ after the $20e/Å^2$ contour. Dashed contour at $4e/Å^2$. Orientation of the polyion is shown. Atomic sites are marked: open circles for oxygens or hydroxyl oxygens; spoked circles for water oxygens. Compare to Figs. 3 (text), IIe, IIh and IIi.

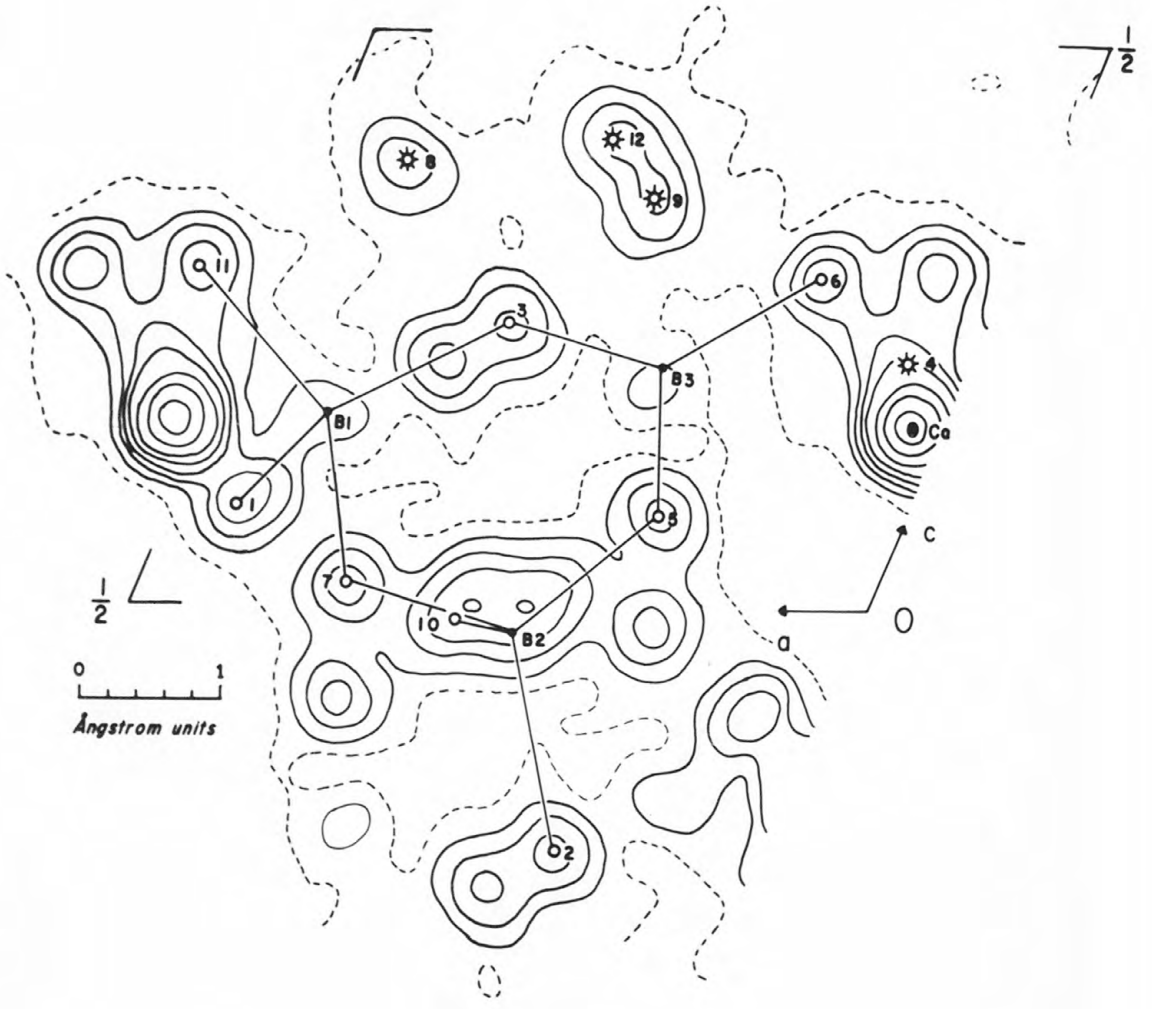

Figure III a

Figure IIIb

Final $\rho_x(y,z)$. Contours at intervals of 4e/Å^2 except around Ca where intervals become 10 e/Å^2 after the 20e/Å^2 contour. Dashed contour at 4e/Å^2. Orientation of the polyion is shown. Atomic sites are marked: open circles for oxygens or hydroxyl oxygens; spoked circles for water oxygens. Compare to Fig. IIf.

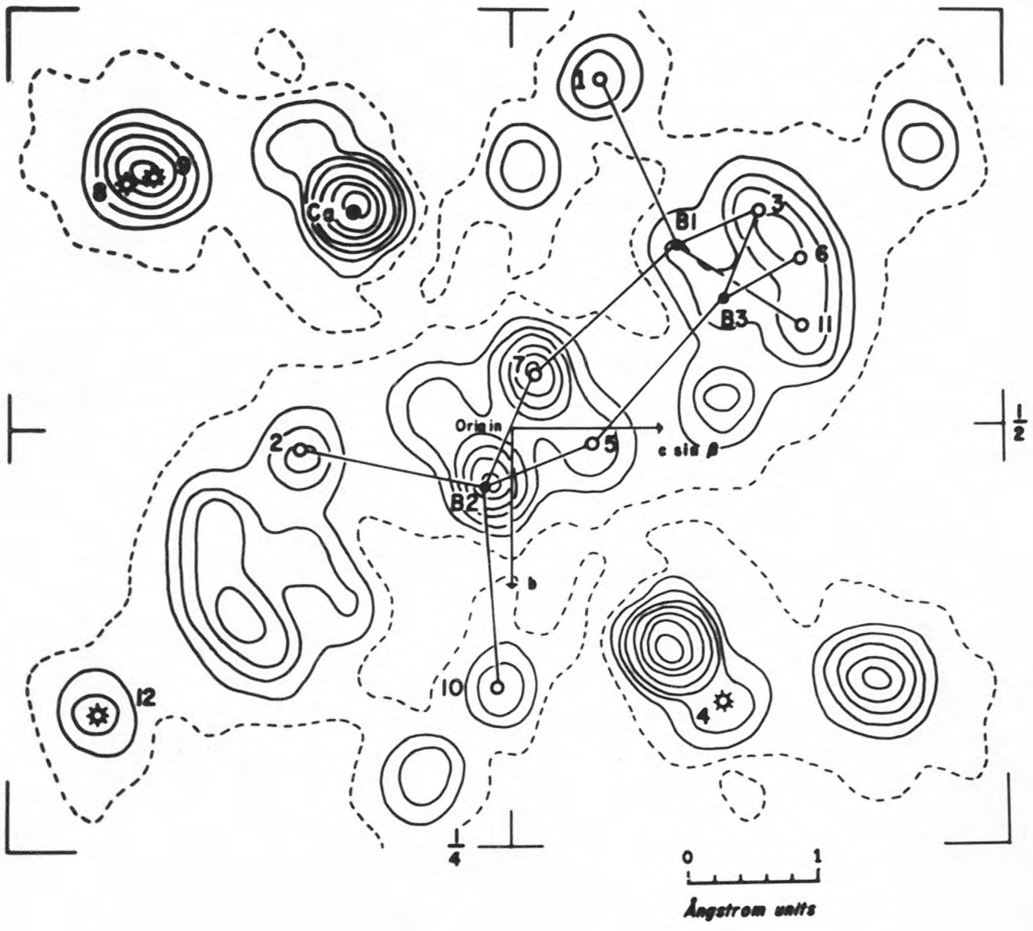
1
3
6
11
B1
B3
B2
7
5
2
12
10
4
Origin
c sin β
b
1/2
1/4
0
1
Ångstrom units

Figure III b

Appendix IV

Use of Difference Syntheses for Structure Refinement

For most crystal structures the preliminary refinement of atomic coordinates is carried out by successive electron-density syntheses, each containing additional terms. The end of this refinement process is reached with the electron-density calculation which includes all (or nearly all) of the F_o. Least-squares treatment of the data is often the next refinement procedure, especially when high-speed machine computing facilities are available.

An alternative refinement method uses difference syntheses, $D = \rho_o - \rho_c$, which are calculated in the same way as the corresponding electron-density projections (Appendix III), except that $(F_o - F_c)$ values are the series coefficients. Lipson and Cochran (1953) have shown that a D synthesis leads to the same atomic coordinates that would be given by least-squares calculations if the weighting factor for the latter were $1/\hat{f}$ for all observations $\left\{\hat{f} = \sum_{j=1}^{N} f_j \Big/ \sum_{j=1}^{N} Z_j\right\}$. Adjustment of previously assigned temperature factors and atomic scattering factors may also be made from D maps in the later stages of refinement.

To study a D synthesis, contours of constant D are plotted and atomic positions used in the previous S.F. calculations are marked. The position of a correctly located atom is found in a region of nearly zero slope, while incorrectly located positions lie on steeper slopes. Indicated shifts in atomic positions can be estimated by moving along the perpendicular to the D-contour through the atomic center, in the direction of increasing D, an amount proportional to the separation of the contour lines near the atomic center.

These principles were applied to refinement of the inyoite structure. Numerous overlapping atoms in the projection on a plane normal to [100] precluded its use, but both $D_z(x,y)$ and $D_y(x,z)$ were calculated from S.F. based on the atomic coordinates of Table 2, column 3 (text). The resulting D maps are shown in Figs. IVa and IVb. For each atom the initial position has been marked with a cross and the direction of movement indicated by an arrow. The magnitude of the shifts can be found by comparing the final coordinates (Table 2, column 4) with the previous ones (Table 2, column 3).

After the next set of S.F. (Table 3), a second pair of D maps was examined. While these have not been reproduced here, they showed most of the atomic positions now lying in or near regions of small slope. Assignment of individual temperature factors is indicated as the next step in the refinement procedure. When the three-dimensional data are refined by least-squares techniques, this step will be carried out.

Figure IVa

$D_z(x,y)$ No. 1. Dotted contour at zero, others at invervals of 0.4e/Å^2 with dashed contours for negative regions. Atomic positions are marked with crosses and arrows indicate shift directions.

Figure IV a

Figure IVb

$D_y(x,z)$ No. 1. Dotted contour at zero, others at intervals of 0.4e/Å^2 with dashed contours for negative regions. Atomic positions are marked with crosses and arrows indicate shift directions.

Figure IV b

Appendix V

Use of the Hauptman-Karle Σ_1 Relationship

Probability relationships for phase determination in centrosymmetric crystals were first developed and given a general treatment by Hauptman and Karle (1953). These relationships permit sign determination from calculations which initially involve only magnitudes of the normalized structure factors, E_o. For inyoite all E_o contained within the sphere of radius $s = (\sin\theta)/\lambda = 0.9$ Å were calculated from the relative $F_{hk\ell}$ by using the relationship $E^2_{hk\ell} = [K(s)F^2_{hk\ell}\ ]/\varepsilon\sigma_2$, where $\sigma_2 = \sum_{j=1}^{N} f_j^2$ and ε is a factor dependent on the space group. For $\underline{P}2_1/\underline{a}$ $\varepsilon = 2$ for $hk\ell$ having $h = \ell = 0$ or $k = 0$, while for all other $hk\ell$, $\varepsilon = 1$.

The probability relationship from which the Σ_1 equation is derived may be written as follows:

$$P_+(F_{h'k'\ell'}) = \frac{1}{2} + (\text{coef.})|E_{h'k'\ell'}|(E_{hk\ell} - 1),$$

where $P_+(F_{h'k'\ell'})$ is the probability that the sign of $F_{h'k'\ell'}$ is positive and where $h' = 2h$, $k' = 2k$, $\ell' = 2\ell$. The coefficient is a function of the atomic numbers for the atoms of the particular structure being investigated.

In space group $\underline{P}2\ /\underline{a}$ the Σ_1 equation is:

$$S_{h'0\ell'} = \sum_k (-1)^{h+k}(E_{hk\ell} - 1),$$

where $S_{h'0\ell'}$ is the probable sign associated with $F_{h'0\ell'}$ and $h' = 2h$, $\ell' = 2\ell$. It was possible to evaluate this equation for a given $h'0\ell'$ of inyoite in about ten minutes with the aid of a desk calculator. The Σ_1 sum was therefore formed for 22 $h'0\ell'$ terms with $|E_{h'0\ell'}|>1.000$, a large $|E_{h'0\ell'}|$ being desirable because of its favorable effect on $P_+(F_{h'0\ell'})$. In order to decide from the Σ_1 magnitude whether an $h0\ell$ sign could be accepted, the requirement, $|\Sigma_1|>3(n)^{1/2}$, was made, n being the number of terms contributing to the sum. Generally the inyoite sums included about 18 contributors so the requirement became $|\Sigma_1|>13$.

Of the 22 terms examined, seven signs were statistically acceptable and checked those already assigned on the basis of the contribution of the Ca atom to the structure factors. No further use was made of the Hauptman-Karle relations because additional information about signs of $hk\ell$ terms with one zero index could not be obtained from other sign relationships without completing a full three-dimensional sign determination. Two sample Σ_1 calculations are given below, one for the 602 term, the sign of which was correctly determined as negative by the statistical criteria, and one for the 806 term, the sign of which was indeterminate by the statistical criteria (later calculated from the structure as positive).

Table Va

Σ_1 calculation for 602 ($|E|$=1.703)

hkℓ	$(-1)^{h+k}$	$E^2_{hk\ell}-1$	π^*	Σ_1
311	+	-1.000	-1.000	
321	-	1.531	-1.531	
331	+	-0.341	-0.341	
341	-	-0.589	0.589	
351	+	-1.000	-1.000	
361	-	2.338	-2.338	
371	+	-0.930	-0.930	
381	-	0.621	-0.621	
391	+	1.008	1.008	
3,10,1	-	7.294	-7.294	
3,11,1	+	-0.810	-0.810	
3,12,1	-	-0.069	0.069	
3,13,1	+	-0.950	-0.950	
3,14,1	-	2.049	-2.049	
3,15,1	+	-1.000	-1.000	
3,16,1	-	1.158	-1.158	
3,17,1	+	-1.000	-1.000	
3,18,1	-	-1.000	1.000	
3,19,1	+	-1.000	-1.000	
3,20,1	-	3.700	-3.700	
3,21,1	+	-1.000	-1.000	-25.056

*$\pi=(-1)^{h+k}(E^2_{hk\ell}-1)$

Table Vb

Σ_1 calculation for 806 ($|E|$=2.290)

hkℓ	$(-1)^{h+k}$	$E^2_{hk\ell}-1$	π^*	Σ_1
403	+	-0.665	-0.665	
413	-	0.711	-0.711	
423	+	-0.701	-0.701	
433	-	0.109	-0.109	
443	+	0.390	0.390	
453	-	-1.000	1.000	
463	+	-0.010	-0.010	
473	-	-1.000	1.000	
483	+	-0.690	-0.690	
493	-	-1.000	1.000	
4,10,3	+	-1.000	-1.000	
4,11,3	-	0.402	-0.402	
4,12,3	+	-0.252	-0.252	
4,13,3	-	-1.000	1.000	
4,14,3	+	-0.441	-0.441	
4,15,3	-	-0.222	0.222	
4,16,3	+	1.137	1.137	
4,17,3	-	-1.000	1.000	
4,18,3	+	0.479	0.479	
4,19,3	-	1.068	-1.068	1.179

*$\pi=(-1)^{h+k}(E^2_{hk\ell}-1)$

References for Appendices

Buerger, M. J. (1951). Acta Cryst. 4, 531.

Harker, D. (1936). J. Chem. Phys. 4, 381.

Hauptman, H. and Karle, J. (1953). Solution of the Phase Problem. I. The Centrosymmetric Crystal. ACA Monograph No. 3. Wilmington: The Letter Shop.

James, R. W. (1954). The Crystalline State, Vol. II. The Optical Principles of X-Ray Diffraction. London: G. Bell and Sons, Ltd.

Karle, J. and Hauptman, H. (1953). Acta Cryst. 6, 473.

Lipson, H, and Cochran, W. (1953). The Crystalline State, Vol. III. The Determination of Crystal Structures. London: G. Bell and Sons, Ltd.

Patterson, A. L. (1935). Zeits. f. Krist. (A)90, 517.